A unified view on catalytic conversion of biomass and waste plastics

Kyungho Lee[1,3], *Yaxuan Jing*[1,2,3], *Yanqin Wang*[2] ✉ *and Ning Yan*[1] ✉

Abstract | Originating from the desire to improve sustainability, producing fuels and chemicals from the conversion of biomass and waste plastic has become an important research topic in the twenty-first century. Although biomass is natural and plastic synthetic, the chemical nature of the two are not as distinct as they first appear. They share substantial structural similarities in terms of their polymeric nature and the types of bonds linking their monomeric units, resulting in close relationships between the two materials and their conversions. Previously, their transformations were mostly studied and reviewed separately in the literature. Here, we summarize the catalytic conversion of biomass and waste plastics, with a focus on bond activation chemistry and catalyst design. By tracking the historical and more recent developments, it becomes clear that biomass and plastic have not only evolved their unique conversion pathways but have also started to cross paths with each other, with each influencing the landscape of the other. As a result, this Review on the catalytic conversion of biomass and waste plastic in a unified angle offers improved insights into existing technologies, and more importantly, may enable new opportunities for future advances.

[1]*Department of Chemical and Biomolecular Engineering, National University of Singapore, Singapore, Singapore.*

[2]*Key Laboratory for Advanced Materials and Joint International Research Laboratory of Precision Chemistry and Molecular Engineering, Research Institute of Industrial Catalysis, School of Chemistry and Molecular Engineering, East China University of Science and Technology, Shanghai, China.*

[3]*These authors contributed equally: Kyungho Lee, Yaxuan Jing.*

✉*e-mail: wangyanqin@ecust.edu.cn; ning.yan@nus.edu.sg*

https://doi.org/10.1038/s41570-022-00411-8

Use of biomass and waste plastic holds promise to aid the global agenda of pursuing a carbon-neutral and waste-free human society. Biomass refers to a broad range of natural organic materials, either plant-based or animal-based that are potential chemical and energy fuel sources. Potentially 240 EJ per year (1 EJ = 24 Mt of oil equivalent) of energy can be delivered from wood harvesting, agriculture and municipal waste by 2060[1], although at present, the portion of biomass-derived energy used in industrial consumption is still small (for example, ~9% in the EU in 2017)[2]. Biomass-derived chemicals make up an increasing share of the global chemical market, projected to reach 22% in 2025[3].

Plastics are artificial substances that have made an incredible contribution to the development of mankind. However, most plastics use petroleum-derived synthetic polymers as main ingredients, raising major environmental concerns[4,5]. Of all the plastic ever made (8,600 Mt), 59% of it has been discarded, ending up in landfills or accumulated in the natural environment such as oceans, and only 17% has been recycled or incinerated to recover energy[6]. The amount of waste plastic has increased tremendously recently due to lifestyle changes caused by COVID-19 restrictions; the use of packaging plastic grew more than 10% globally over the past 2 years (from 2019 to 2021)[7]. The improved handling of waste plastic through processes such as upcycling has never been more important.

By taking a close look into biomass and plastics, one can recognize their substantial compositional and structural similarities at the macroscale and microscale (FIG. 1). If we compare a piece of wood and a disposable mask (FIG. 1a), both are composite materials with secondary interactions among polymer chains such as hydrogen bonding and crosslinking. The secondary interactions between different types of polymers, such as between cellulose and lignin, are important properties of raw biomass and waste plastics[8]. These interpolymer interactions heavily influence the characteristics of the polymer and often add resistance to chemical decomposition, or recalcitrance (FIG. 1b). In addition, the molecular structures of biomass and plastics reveal similar elemental compositions, mainly C, O, N and H, and framework connectivities, primarily relying on C–C, C–O and C–N linkages (FIG. 1c). Although the transformation of biomass and plastic waste into value-added products have been paid considerable attention in the twenty-first century, they are most often studied and reviewed separately in the literature (biomass[9–16], plastic waste[17–22]). However, the substantial structural similarities between biomass and plastic results in striking similarities between the two feeds in bond activation chemistry and catalytic conversion. As such, biomass and plastic share common conversion strategies both in the past and at present.

Non-catalytic thermochemical technologies have been developed as major strategies to transform biomass

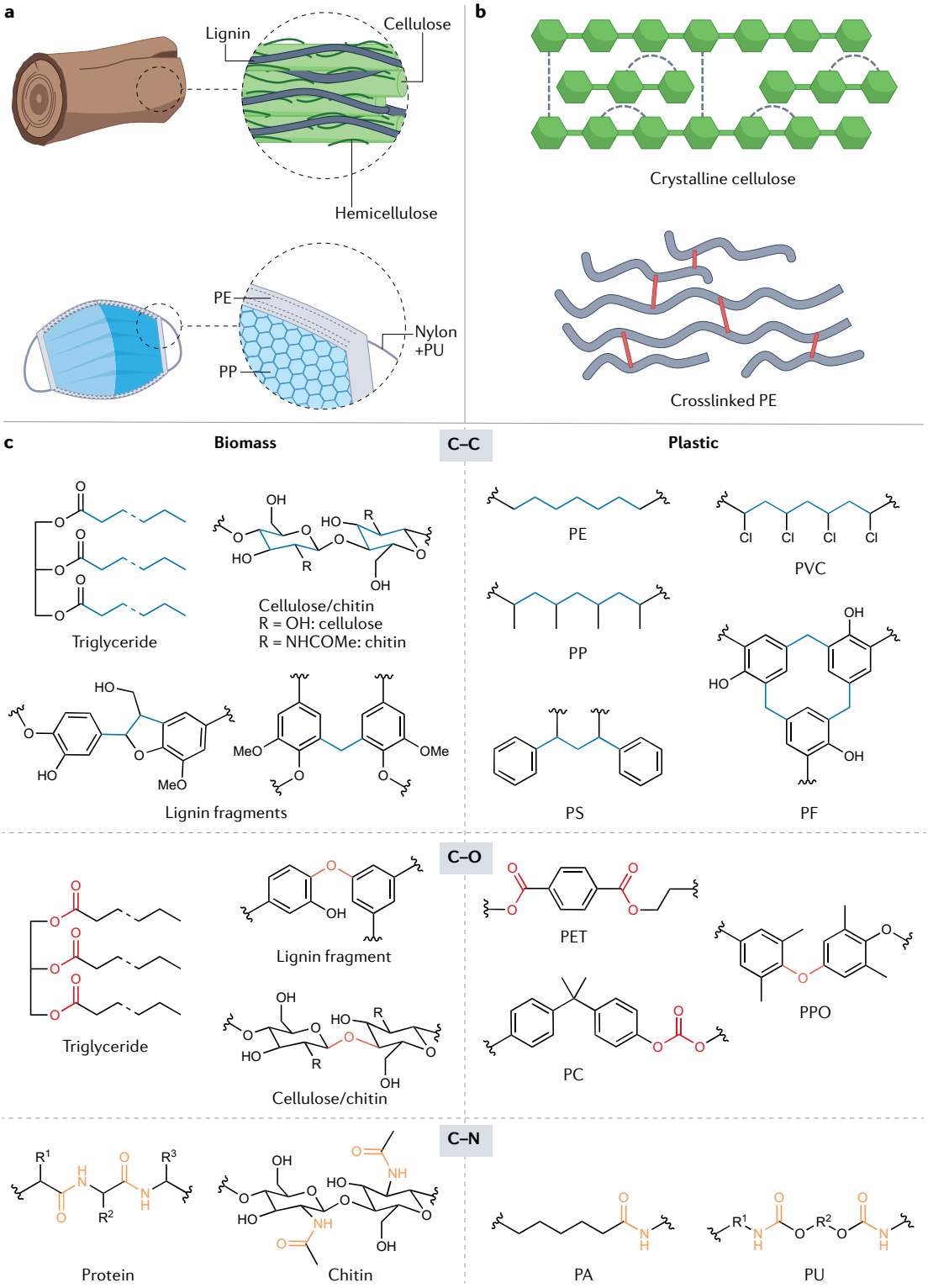

and plastic wastes into chemicals, heat, electricity and materials. Thermochemical technologies for biomass and waste plastics are summarized in BOX 1. One limitation of these approaches is that they are 'non-selective'. To get high-quality fuels and chemicals, both pyrolysis and gasification products from biomass and plastics require substantial further upgrading. Catalysts improve the process economics by shifting the reaction conditions to milder temperatures and lower pressures. In addition, they enhance selectivity towards the desired product. In recent years, there has been substantial academic interest in exploring catalytic transformation of these organic polymeric feedstocks beyond solely thermal technologies. The energy industry and policymakers have also devoted considerable effort to promote catalytic technologies for handling renewable feedstocks.

◀ Fig. 1 | **Chemical similarities between biomass and plastics. a** | Composition and macro-structures of woody biomass and disposable face masks. Woody biomass is mostly composed of cellulose, hemicellulose and lignin, together with a small amount of protein, lipid and other minor components, whereas disposable masks are made from polyethylene (PE), polypropylene (PP), nylon and polyurethane (PU). **b** | Secondary interaction in biomass and plastics. Hydrogen bonding in cellulose and crosslinking among chains in PE make polymers more recalcitrant. **c** | Chemical structure of representative biomass and plastic components. Biomass and plastics show similarities in C–C, C–O and C–N bond linkages. C–C bonds are the dominant linkages in several important plastics such as PE, PP, polyvinyl chloride (PVC), polystyrene (PS) and phenol formaldehyde resin (PF). It also commonly exists in lignin and fatty acid chains. C–O linkages are similarly prevalent. Monosaccharide units in cellulose, hemicellulose and chitin are exclusively connected by glycosidic bonds, whereas phenolic monomers are linked together by ether bonds to form lignin or polyether plastics. Ester linkages are commonly found in triglycerides and polyester such as polyethylene terephthalate (PET). C–N linkages widely exist in proteins, as well as polyamides (PAs) and PU. PC, polycarbonate; PPO, poly(*p*-phenylene oxide).

Here, we attempt to display the catalytic conversion of biomass and waste plastics in a unified angle, summarizing various technologies in the selective degradation and bond activation chemistry of the two feedstocks. This Review starts by describing different conversion strategies, in particular with respect to recently developed catalytic systems that are able to precisely activate C–C, C–O and C–N linkages. Instead of treating biomass and plastics as different feedstocks, representative examples from both areas are grouped together should they share similar chemical transformation in nature. This is especially emphasized in bond activation chemistry and associated catalyst design strategy, with various heterogeneous and homogeneous catalytic systems selected as examples. The intention of this Review is not to provide a full collection of publications, but to offer a clear illustration of the chemistry, provide improved insights into existing approaches and potentially aid in the discovery of new opportunities. Readers may refer to excellent reviews to get a more comprehensive understanding on biomass[9,11,13,23] and plastic[18–21,24,25] conversion. Reviews on specific catalytic pathways such as thermocatalytic[10,26–29], electrocatalytic[30], photocatalytic[12,14,15] and enzymatic[19,31] to convert biomass or plastics are also well documented.

Conversion through C_{aliph}–C_{aliph} cleavage

The C–C bond, including C_{aliph}–C_{aliph} and C_{arom}–C, is ubiquitous in biomass and plastics. As shown in FIGS. 1c and 2a, aliphatic carbon chains exist in natural oils (triglycerides), polysaccharides, lignin and in numerous thermoplastics such as polyethylene (PE; global production of 125 Mt per year)[20] and polypropylene (PP; global production of 69 Mt per year)[20]. Polyvinyl chloride (PVC; global production of 39 Mt per year)[20] is a special class of plastic containing a halogen. It is proposed that dechlorination is required before depolymerization as the presence of chlorine contaminates the products as well as poisons catalysts. Thus, the depolymerization chemistry of PVC is similar to that of polyolefinic plastics. In general, C–C bonds in non-substituted aliphatic chains (C_{aliph}–C_{aliph}) have a high dissociation energy (~370 kJ mol^{-1}) and are rather inert (FIG. 2a), whereas in substituted aliphatic carbon chains such as in the case of glucose and PP, the bond dissociation energy can be lower than 300 kJ mol^{-1}. Three catalytic technologies to cleave C_{aliph}–C_{aliph} bonds have received considerable interest, including catalytic cracking over a solid acid catalyst (for example, zeolite), hydrogenolysis over a metal catalyst and hydrocracking over a metal-acid bifunctional catalyst. These strategies have been well developed in oil refineries to convert heavy petroleum feedstocks into valuable shorter chain products. For biomass and waste plastic conversion, several commercial-level processes such as Anellotech's Bio-TCat (woody biomass and waste plastics to benzene, toluene, xylenes and/or fuels)[32], Shell's integrated hydropyrolysis and hydroconversion (IH^2; non-food biomass and municipal wastes into hydrocarbons)[33], Neste's NExBTL technology (vegetable oils to renewable diesel and aviation fuel)[34] and Honeywell UOP's ecofining process (triglycerides to liquid fuels)[35] have recently been developed. Transformation pathways beyond thermal cracking have also been explored.

Catalytic cracking. Catalytic cracking is conducted at high temperature in the presence of a Brønsted acid catalyst (for example, zeolite), ideally aiming to produce gasoline-range hydrocarbons and light olefins (C_2–C_4) (FIG. 2b). Two types of scission, protolytic cracking (monomolecular cracking) and β-scission (bimolecular cracking), are involved in C–C cleavage chemistry. Considering that β-scission can only produce ≥C_3 hydrocarbons[36], and protolytic cracking has a higher activation energy than β-scission[37,38], increasing reaction temperature leads to dominant production of light hydrocarbons (for example, methane, ethane and ethylene). As a compromise between activity and liquid product selectivity, fluidized catalytic cracking (FCC) processes are conducted at around 500 °C. Repeated catalyst regeneration at 700 °C using steam is essential, due to fast coke deactivation[39]. Ultrastable Y zeolite (USY) has been identified as the optimal catalyst due to its superior liquid oil production activity and steam tolerance. Zeolite Socony Mobil-5 (ZSM-5) is able to produce light olefins and aromatics owing to its 10-membered ring micropore structure. Catalytic cracking is not limited to solid raw feedstocks, but can also be widely adopted to secondary-step technologies, such as upgrading of pyrolysis oils or vapours.

According to a report from UOP[40], vegetable oil could be transformed to fuel (gasoline and diesel) and olefins with similar yields (olefin process: 22 wt%, gasoline process: 45 wt%) and an insignificant coke formation (≤6.5 wt%) to those obtained from industrial vacuum gas oil (VGO). However, bio-oil and lignin produce a notable amount of coke (bio-oil: 10–20 wt%, lignin: 15–50 wt%, respectively)[41–43]. Owing to a high oxygen content in bio-oil and lignin, the accompanied hydrodeoxygenation reduces the amount of intramolecular hydrogen promoting coke formation. In the case of lignin, repolymerization of the phenolic monomer is another factor to form coke[44]. Conversely, when glycerol is co-fed with VGO into the reactor, the product mixture has a higher olefin to paraffin ratio than using pure VGO, which is desirable in the refinery industry[45], thus increasing the efficiency of catalytic cracking processes. Further investigations on how the oxygenates change the reaction pathway, stabilize the olefinic intermediates on

Box 1 | **A glance at non-catalytic thermochemical technologies for biomass and plastic conversion**

The conversion of biomass and waste plastic requires high temperatures. Heating promotes the decomposition of feedstocks into small fragments. The associated technologies are classified by their operation temperature and gas atmosphere.

Pyrolysis converts feedstocks into gases, liquid oils and solid residues by heating at 400–700 °C in the absence of oxygen[214–219]. The product (gas, liquid, and solid) distribution is highly dependent on the reaction temperature (thermodynamics), as well as heating/cooling rates (kinetics). As the major goal is to maximize bio-oil fraction (that is, liquefaction)[214], recent developments focus on flash/fast pyrolysis (heating rate of >1,000 °C s^{-1}, residence time of <1 s)[216]. Nonetheless, gas or solid products can be also targeted if the economic factors are feasible.

Gasification converts feedstocks into mainly CO, CO_2 and H_2 through high temperature (>700 °C) treatment by using a controlled amount of oxygen or steam[220–225]. Practically, the key factor in gasification is minimizing residue (that is, tar) formation and increasing the gas yield. Maximizing the yield of H_2 is also a major goal for process efficiency[221].

Carbonization generally means the production of solid carbon (that is, (bio)char) via slow pyrolysis (residence time: hours to days). Further activation and structuring produces functional carbon nanomaterials[226,227]. Alternatively, light gases produced through gasification can be used as carbon precursors. Chemical vapour deposition of light gases is widely used, especially for carbon nanotube synthesis[226]. Biomass and plastic wastes have a lot of potential for the synthesis of functional carbon material due to the presence of heteroatoms (for example, O and N) in their structures[228].

Biomass and waste plastics can be co-fed into pyrolysis and gasification units, implying compatibility between the two feedstocks. Generally, the product distribution is highly affected by the C to O ratio, especially for pyrolysis. Gasification is not substantially affected by the type of feedstock because of its higher reaction temperature resulting in complete decomposition of feedstocks.

the catalyst surface, as well as change the thermodynamics and fluid dynamics are necessary. In the case of plastic catalytic cracking, diverse substrates such as PE, PP and PS were transformed to 70–80 wt% yield of liquid oil with similar fuel specifications to conventional diesel[28]. A recent study on PP catalytic cracking using industrial FCC catalysts found that poisoning by metal impurities and steaming, which are known to be harmful to zeolite catalyst, oppositely enhanced aromatics selectivity and suppressed coke formation[46]. It should be noted that industrial FCC catalysts are specially optimized for petroleum-derived feedstocks, thus opportunities exists to develop catalysts and processes tailored for biomass and plastic feedstocks.

Hydrogenolysis. Hydrogenolysis using metal catalysts is another facile C_{aliph}–C_{aliph} cleavage strategy. For waste plastic in particular, this strategy has reached commercial plant operation scales[47]. Hydrogenolysis of PE in the presence of a Ru/C catalyst produced ~40 wt% of C_8–C_{45} and 50 wt% of C_1–C_7 hydrocarbons, with CH_4 being the most abundant product[48]. It is an enduring problem that H_2 is not cheap but hydrogenolysis predominantly produces relatively low-value short-chain linear paraffins (FIG. 2c). Hence, developing innovative pathways to produce more valuable longer-chain products with a decreased H_2 consumption is essential.

To this end, a 2 nm Pt-dispersed $SrTiO_3$ catalyst was introduced to transform PE into lubricant and wax products with a uniform C-number distribution[49]. The uniform product distribution is attributed to more favourable adsorption of PE and high-molecular-weight fragments on Pt rather than $SrTiO_3$. More recently, a novel catalyst mimicking the behaviour of enzymes, that is, processive polymer deconstruction, was reported to efficiently transform PE into valuable liquid products[50]. The catalyst has a specially designed architecture, composed of Pt nanoparticles housed in ordered mesoporous SiO_2 ($mSiO_2$) with a pore 2.4 nm in diameter and 110 nm in length. The $mSiO_2$ grasps the PE chain so that the polymer is only mobile in a narrow channel. Thus, PE is adsorbed onto the Pt site at the inner end of the pore in a straightened conformation. This confined adsorption mode sequentially leads to selective cleavage of the C–C bonds and release of short-chain products, producing a more uniform product profile than those obtained from open-structured Pt catalysts, which is desirable for diesel and lubricant applications.

Hydrogenolysis can be combined with secondary processes to give rise to new conversion pathways. For example, one-pot hydrogenolysis–aromatization of PE waste was successfully demonstrated[51] (FIG. 2d). Two reactions with different thermodynamic natures, that is, exothermic hydrogenolysis and endothermic aromatization, were elegantly coupled together at a moderate temperature (280 °C) using a common Pt/γ-Al_2O_3 catalyst. As the hydrogen generated via aromatization is sufficient to sustain the first hydrogenolysis step, no external H_2 supply is required. Remarkably, highly valuable long-alkyl-chain-functionalized aromatics can be produced over a relatively simple monofunctional Pt catalyst.

Hydrocracking. Triglyceride has a low oxygen content compared with other biomass and the length of its fatty acid chain is similar (C_{14}–C_{22}) to those of diesel and jet fuel. Hydroconversion of triglyceride has been successfully industrialized to produce biofuels, in which hydrocracking is a major pathway for the transformation.

Hydrocracking refers to cracking using metal–acid bifunctional catalysts, in which the acid sites promote C–C cleavage, whereas the metal sites facilitate the paraffin–olefin transition in the initiation and termination steps. It is carried out at much lower temperatures (for example, 200–300 °C) than catalytic cracking, so that C–C cleavage occurs almost exclusively via β-scission. Unlike in hydrogenolysis over a metal, branched paraffins are the dominant products because isomerization occurs before β-scission[36]. For the metal component, various Ni, NiMo-sulfide, CoMo-sulfide and noble metals can be used. NiMo-sulfide and CoMo-sulfide have received increasing interest in the past five decades owing to their high hydrogenation activity as well as their cheaper costs than noble metals. However, they require co-feeding of a sulfur source (for example, H_2S) because of the rapid deactivation of the metals from loss of the active metal-sulfide moieties as well as coke deposition[52,53]. For the zeolite component, 12-membered ring zeolites (USY, Beta) are ideal to produce diesel or jet fuel, whereas the narrow pore structure of ZSM-5 limits diffusion of branched hydrocarbons, inducing overcracking[54].

The industrial process for the conversion of triglyceride into green diesel and jet fuel (Ecofining, Honeywell UOP) comprises a multistep process[35,55] ((1) in FIG. 2e): hydrogenolysis–deoxygenation of triglyceride into

linear paraffins in the first reactor using a metal catalyst, separation of inorganic gases (CO, CO_2 and H_2O) and hydrocracking of linear paraffins to branched paraffins at the second reactor using a metal–acid catalyst. Naphtha (13 wt%), aviation fuel (55 wt%), diesel (10 wt%) and the rest gas products ($\leq C_4$) are typically obtained after distillation. Controlling product distribution can be easily achieved by a slight change of reaction

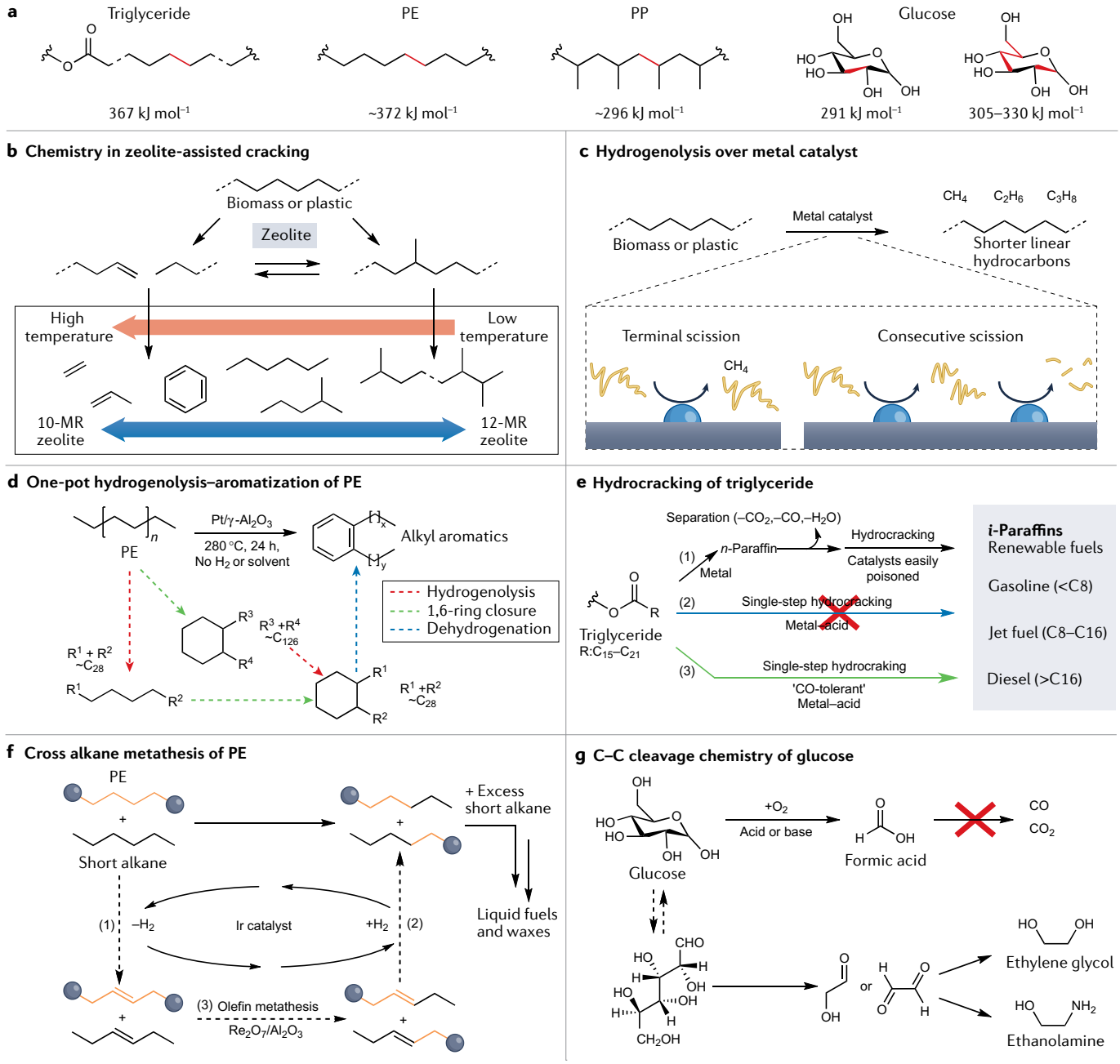

Fig. 2 | **Conversion strategies of C_{aliph}–C linkages in biomass valorization and plastic upcycling. a** | Bond dissociation energy of various C_{aliph}–C bonds in biomass and plastics.† **b** | Catalytic cracking over a zeolite catalyst. Product distribution is controlled by reaction conditions and crystalline structure of the zeolite. **c** | Hydrogenolysis over metal catalyst. Terminal and consecutive scission of the polymer substrate induces the production of shorter linear hydrocarbons. **d** | One-pot hydrogenolysis–aromatization of polyethylene (PE) using Pt/γ-Al_2O_3 catalyst[51]. The process was achieved via sequential hydrogenolysis and 1,6-ring closure, followed by dehydrogenation. **e** | Hydrocracking of triglycerides in a single-step conversion process to produce transportation fuels could be achieved by CO-tolerant metal–acid bifunctional catalysts. **f** | Cross alkane metathesis of PE, which occurs through dehydrogenation, metathesis and hydrogenation, to form liquid fuels and waxes. The Ir catalyst promotes dehydrogenation and hydrogenation, whereas the Re_2O_7/Al_2O_3 catalyst is responsible for metathesis[78]. **g** | C–C cleavage chemistry of glucose. Oxidative cleavage offers formic acid, whereas retro-aldol condensation leads to C_2–C_4 products, which can be further upgraded into ethylene glycol and ethanolamine. †The bond dissociation energies were calculated with density functional theory using the Vienna Ab initio Simulation Package with the Perdew–Burke–Ernzerhof functional for describing the exchange correlation of electrons. The structure was optimized until the maximal force residue was below 0.02 eV Å^{-1} and the energy difference between iterations was smaller than 1.0 e^{-6} eV^{-1}. The cut-off energy for the plane-wave basis was set to 520 eV and spin polarization was considered. Some values are expressed as averages, accounting for the various molecular weights of the polymers. MR, membered ring; PP, polypropylene.

temperature; thus, catalyst development to improve activity and selectivity do not seem to be urgently demanded.

Conversely, there are still opportunities for catalyst design to contribute to an improved process intensification. In 2021, Honeywell UOP announced the success of an advanced triglyceride-to-fuel technology, which reduced complex multistep reactions to a single step[56]. Although the composition of industrial catalysts is veiled, the catalyst design concept to achieve this process has also been proposed in the literature[57]. In principle, hydrogenolysis and deoxygenation in the first reactor followed by hydrocracking in the second reactor could be carried out using a single reactor because the hydrocracking catalyst itself (for example, Pt/USY) contains metal sites to promote deoxygenation and hydrogenolysis of triglyceride. However, the conversion of triglyceride to jet fuel using a single reactor was not successful[54,57] ((2) in FIG. 2e). This is because there is a quantitative metal–acid balance criterion for ideal hydrocracking catalyst[58,59], but CO generated during deoxygenation poisons the metal site causing a metal–acid imbalance in the bifunctional catalyst. This led to severe overcracking and coke formation during triglyceride conversion. To combat this, a CO-resistant, bimetallic PtRe/USY catalyst was developed for the direct conversion of triglyceride[57] ((3) in FIG. 2e). This tailor-designed catalyst enabled a single-step hydroconversion of triglyceride into purified jet fuel with 41 wt% yield, highlighting the necessity to design specific catalysts for biomass and plastic conversion rather than simply searching the catalyst toolbox established in petroleum refinery. With synergistic efforts from academia and industry, this area could be developed further.

Hydrocracking is known to be effective to valorize waste PE, PP, polystyrene (PS; FIG. 1c) and their mixtures[60]. For instance, hydrocracking of PE produces a large quantity of aromatics, gasoline and light gas regardless of the type of catalyst (for example, Ni(Mo)/silica-alumina, NiMo/zeolite, Pt/WO_3/ZrO_2 and Pt/USY)[61–64]. This implies the transformation comprises parallel pathways including catalytic cracking, hydrogenolysis and aromatization. To achieve selective hydrocracking to produce valuable fuel-like products, the reaction mechanism and structural requirements of the catalyst need to be investigated in detail. A recent report on hydrocracking of PE using a Pt/WO_3/ZrO_2-mixed USY catalyst system gave improved insights[65]; acidic WO_3/ZrO_2 is not simply a support for Pt, but it breaks the polymer into C_{13+} hydrocarbons, which subsequently react on USY to produce gasoline-range hydrocarbons (C_5–C_{12}). The skeletal structure of the substrate also fundamentally affects reactivity. PP, which contains branches, produces fewer products with shorter carbon chains and results in a higher isomer ratio than PE under the same conditions and catalyst[65,66]. This feature implies that C–C scission in PP is predominantly processed via hydrocracking, presumably due to the easier formation of the branched-carbenium intermediate. In other words, PP is a promising feedstock to be converted into transportation fuels (especially jet fuel and diesel). Waste plastics, unlike crude oil or triglyceride-derived sources, require multiple C–C cleavages, and thus the validity of the classical metal–acid balance criterion should be reconsidered. Zeolites have a narrow micropore aperture (<1 nm), thus only the external surface can work efficiently for plastics that have large molecular sizes. In this regard, hierarchical zeolites, allowing faster molecular diffusion, have been proven to be beneficial for various acid catalyses of biomass and plastics including hydrocracking[27,39,54,67–69]. As hierarchical zeolites have very different properties, such as shape selectivity[70] and acid strength[71], from bulk zeolites, investigation on reaction mechanism and structural criteria of bifunctional catalysts, particularly in plastic conversion, is an urgent issue that needs to be addressed.

Metathesis. As vegetable oil contains C=C bonds in its fatty acid chain, numerous transformation pathways based on alkene metathesis have been considered for triglyceride and its derivatives (for example, fatty acid and fatty ester)[72–74]. For metathesis, homogeneous Grubbs catalysts and Grubbs–Hoveyda catalysts are mostly used, but heterogeneous Re-based catalysts can also be used[75,76]. Elevance successfully scaled up the first metathesis plant for triglyceride refinery[77], which aims to produce modified triglyceride, unsaturated methyl ester and (α-)olefins using ethylene as a reagent. Recently, decomposition of PE via cross 'alkane' metathesis was introduced as a new approach for plastic upcycling[78,79] (FIG. 2f). Unlike conventional metathesis that exchanges the fragments of a C=C bond among unsaturated substrates, cross alkane metathesis does not require a double bond in the substrate. Instead, it consists of tandem: (1) dehydrogenation of the paraffin to an olefin, (2) cross olefin metathesis, and (3) hydrogenation of the olefin products back to a paraffin sequence[80]. The reaction was achieved by coupling a noble metal catalyst responsible for hydrogenation/dehydrogenation and a metathesis catalyst. Alkane metathesis is attractive from an application perspective, as it only requires cheap paraffin feedstock, whereas hydrogen supply is not required due to the circulation of a stoichiometric amount of hydrogen generated. It is an interesting coincidence that the metathesis, which has historically been found during the polymerization of PE, is now also used to depolymerize PE.

Cleavage of oxygen-linked C_{aliph}–C_{aliph}. When the carbon atom in the C_{aliph}–C bonds are linked with oxygen-containing functionality such as a hydroxyl group and/or carbonyl units, specific C–C cleavage strategies become feasible. In classical organic chemistry, oxidative C–C cleavage occurs when diols bearing hydroxyl groups (–OH) on vicinal carbon atoms are treated with oxidants such as periodic acid. Recently, catalytic systems have been developed to convert sugars into formic acids by cleaving the C–C bond (FIG. 2g). Formic acid was obtained in a 60 wt% yield when glucose was oxidized under the aqueous phase with a polyoxometalate catalyst, whereas a 99 wt% yield of methyl formate was generated when methanol was used in place of water as reaction solvent[81]. In another study, a yield of 91 wt% of formic acid was achieved at room temperature in the presence of H_2O_2 and LiOH (REF.[82]);

the enhanced yield was attributed to the synergistic effect of the base and oxidant, leading to an improved oxidative capacity. Another important reaction is the retro-aldol condensation, which has been broadly applied in the degradation of cellulose-based[83,84] and chitin-based[85] carbohydrates. The unique polyhydroxy aldose units in carbohydrates grant the possibility of the chemical production of polyols/alcohols, and other functional molecules, via retro-aldol transformation[86]. Lewis acid catalysts such as metal chlorides, Ni-W_2C, Sn-C-SiO_2 and zeotype catalysts enable the reaction to take place under a mild hydrothermal condition[87–91]. Considering that an oxygen-linked C–C bond is commonly found in lignin, Waldvogel and co-workers reported electrochemical degradation of Kraft lignin (that is, industrial lignin obtained from Kraft pulp) to aromatic chemicals (vanillin and acetovanillone) in 4.2 wt% yields via selective cleavage of oxygen-linked C–C bond[92]. Although plastics do not contain the same type of such C_{aliph}–C_{aliph} bonds, the preferential upcycling of a polyolefin over oxidative cleavage has been reported[93]. The strategy uses microwave oxidation using nitric acid, predominantly producing C_3–C_7 dicarboxylic acids from PE (carbon efficiency = 37 wt%). This highlights the high reactivity of the O-linked C_{aliph}–C_{aliph} bond, potentially expanding the choices for the depolymerization of polyolefinic plastics.

In short, the prevailing strategy to break the C_{aliph}–C_{aliph} linkages in biomass and plastics is through cracking over acid catalyst, hydrogenolysis over metal catalyst and hydrocracking over metal–acid bifunctional catalyst. Co-generated H_2O and CO via deoxygenation in biomass conversion requires specially designed catalysts that are poison-resistant. Metathesis, traditionally only used for C=C-containing feeds, has now been introduced for upcycling aliphatic PE. This strategy can be extended to the valorization of other paraffinic feeds such as waste animal fat. The special C–C cleavage approach for O-linked C_{aliph}–C_{aliph} is only used for biomass at present; however, it hints at new opportunities such as oxidative C–C cleavage of polyolefinic plastics in the future.

Conversion through C_{arom}–C cleavage

In addition to the C_{aliph}–C_{aliph} linkages discussed above, C_{arom}–C bonds are also prevalent in biomass and plastics. These linkages are further categorized into two types: C_{arom}–C_{aliph} and C_{arom}–C_{arom} bonds. The former is found in several aromatic plastics such as PS, phenol formaldehyde (PF) resins (FIG. 1c) and polycarbonate (PC) (global production of 29 Mt per year (REF.[20]), 5 Mt per year (REF.[94]) and 5 Mt per year (REF.[95]), respectively) and lignin fragments featuring β–1, β–5, α–1 and 5–5′ linkages (FIG. 3a). Additional C_{arom}–C_{aliph} bonds form via condensation of reactive intermediates during delignification in Kraft, sulfite or organosolv pulping processes. In addition, the phenylpropanoid subunits of lignin are rich in C_{arom}–C_{aliph} bonds. Conversely, C_{arom}–C_{arom} bonds are much less common, and are only found in lignin fragments connected by 5–5′ linkages. The 5–5′ linkage is the second most abundant form of lignin linkages after β–O–4, and has the strongest dissociation energy (~480 kJ mol^{-1}) among all common C–O and C–C bonds in biomass and plastics (FIG. 3a).

Catalytic cracking. Catalytic cracking over a zeolite catalyst is effective in the cleavage of C_{arom}–C_{aliph} linkages in lignin and aromatic plastics (PS, PC and PF)[96], although the formation mechanism of aromatics from plastics is still not fully resolved. One possible pathway is that the C_{arom}–C_{aliph} linkages are broken during thermal or hydrothermal cracking, whereas benzene rings are preserved[97]. The second pathway is that the polymer framework first completely deconstructs during thermal and catalytic cracking, after which the small fragments rearomatize in the presence of acid catalysts[98]. ZSM-5, arguably the most well-known aromatization catalyst in oil refinery, also shows superior aromatic selectivity in lignin cracking among zeolites[99]. One representative example is the selective cleavage of the phenolic C_{arom}–C_{aliph} bond in lignin to produce phenol and ethylene (FIG. 3b). Hierarchical ZSM-5 catalysts, with a balanced network of micropores and mesopores, were identified as versatile catalysts for the dealkylation reaction[100]. The result of the catalytic cracking is only weakly dependent on the structures of the feedstocks due to the relatively high reaction temperature (500–800 °C). As C and H atoms in aromatic plastic and biomass may exchange during cracking, co-feeding of the two substrates is an effective strategy to break their C_{arom}–C_{aliph} linkages and increase the yield of aromatic products[101]. For example, Sophonrat et al.[102] found that co-pyrolysis of PS and cellulose favoured the formation of aromatic products compared with that from individual feedstock due to the exchange of C and H atoms between cellulose and PS pyrolysis products.

Reductive cleavage. Hydrogenolysis over supported metal catalysts carries several distinct advantages, including lower reaction temperature, higher yields of aromatic products and prevention of overcracking of the aromatic rings, which is a potential issue in acid catalysis. To this end, a multifunctional Ru/$NbOPO_4$ catalyst was used to break interunit bonds in native/processed lignin (FIG. 3c). Compared with earlier reported catalysts that were only able to cut the C–O linkages, the new catalyst system offered a record-high yield of monocyclic compounds due to its ability to break the C_{arom}–C_{aliph} linkages[103]. The roles of the Ru/$NbOPO_4$ catalyst include: providing a Lewis acid centre for the strong adsorption of benzene rings, acting as a Brønsted acid to protonate and activate the C_{arom}–C_{aliph} bonds, and providing metal sites to enable the dissociation of hydrogen to promote attack of the weakened C_{arom}–C_{aliph} bond. On the basis of a similar design principle, a Ru/Nb_2O_5 catalyst comprising small-sized Ru clusters and surface hydroxyl groups as Brønsted acid sites was also developed to upcycle aromatic plastic waste. PS, PC and a mixture of aromatic plastics underwent selective hydrogenolysis reactions to break the C_{arom}–C_{aliph} linkages, offering aromatics as the major products[104].

The transformation of propyl groups in lignin by a suitable aromatic acceptor to form value-added alkyl aromatic products with the use of zeolite catalysts has

drawn notable attention. For example, using benzene as the aromatic acceptor and a mixture of Au/TiO_2 and H^+-ZSM-5 as catalysts, the alkyl groups were transferred to benzene via an alkylation reaction, generating value-added alkylbenzenes[105]. Although plastics such as PS and polyethylene terephthalate (PET) are also enriched with side-chain alkyl groups (FIG. 1c), the carbons in alkyl groups are normally underused[104,106]. The residual alkyl groups in PET and PS could also be used to generate alkylbenzenes via an acid–catalytic alkylation reaction. The desired catalyst should not only contain metal sites enabling H_2 dissociation and acid species for the C–O/C–C bond activation, but also carry strong Brønsted acid sites to facilitate the alkylation reaction, such as phosphorylated Ru/Nb_2O_5 or a combination of ZSM-5 (the structure is given in FIG. 3b) and Ru/Nb_2O_5 (REFS.[104,107]). Another feasible strategy is to weaken the hydrogenolysis ability of the metal species to slow down this transformation while accelerating the intramolecular cyclization to produce indane and its derivatives[108]. In a similar way, a conspicuous example is to produce indane and its derivates from PS through driving its propyl linkages to undergo intramolecular cyclization. On the basis of studies conducted on lignin[104,108], the tuning of catalytic sites to make the intramolecular cyclization rate comparable with

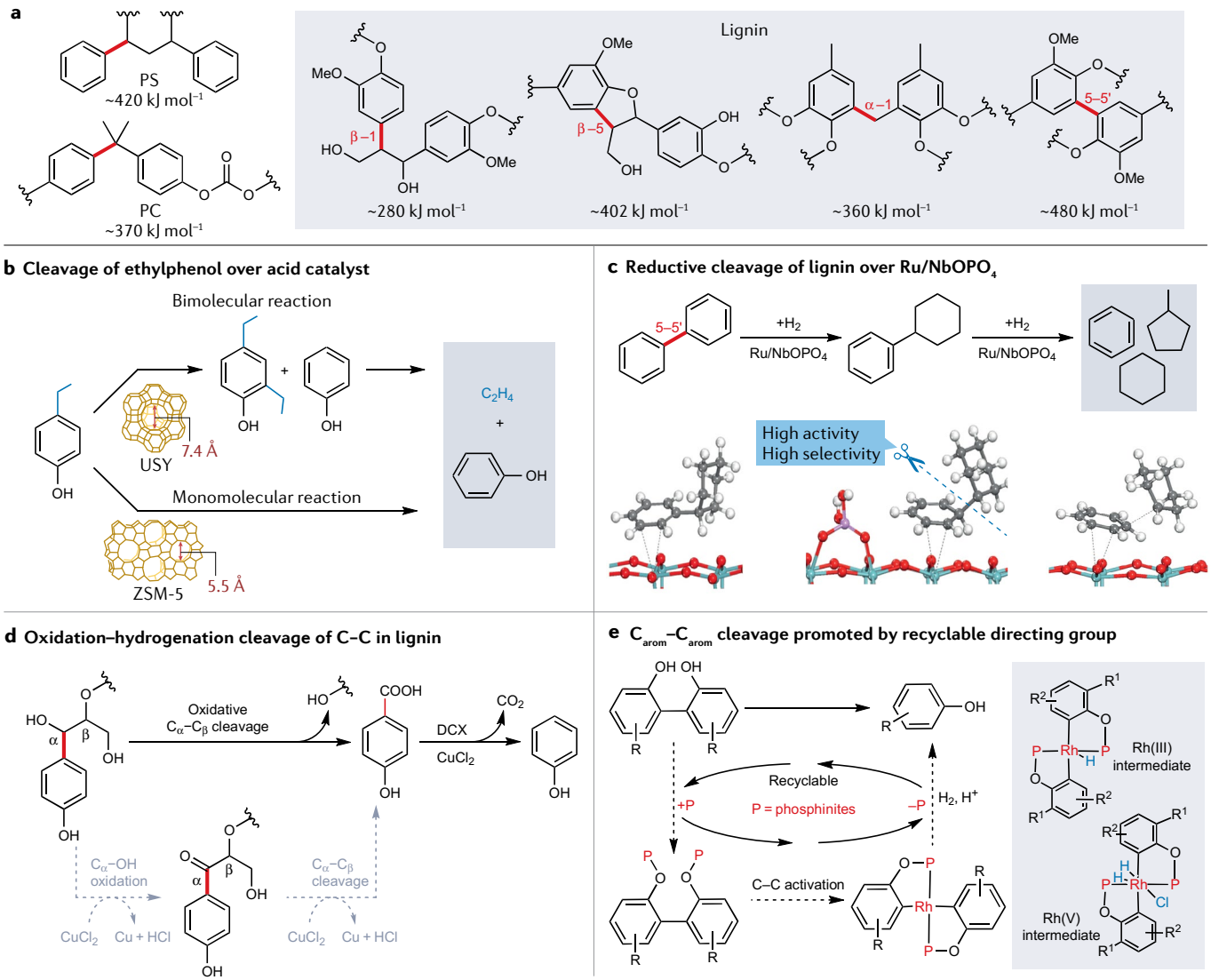

Fig. 3 | **Conversion strategies of C_{arom}–C linkages in biomass valorization and plastic upcycling. a** | Bond dissociation energy of various C_{arom}–C bonds in biomass and plastics. The bond dissociation energies were calculated with density functional theory. The details are described in the footnote † to FIG. 2. **b** | Acid catalysed cleavage of ethylphenol. The structure image shows that the reaction undergoes a bimolecular reaction (disproportionation and cleavage) over unstable Y zeolite (USY), which has a large pore (7.4 Å), but monomolecular reaction (sole cleavage) over Zeolite Socony mobil-5 (ZSM-5), which has a small pore (5.5 Å)[99]. **c** | Reductive C–C cleavage of lignin over Ru/$NbOPO_4$. The catalytic cleavage of 5–5′ linkage is achieved over Ru/$NbOPO_4$ through adsorption, binding, protonation, partial hydrogenation to C_{arom}–C linkages and final cleavage of C_{arom}–C linkages[103,111]. **d** | Oxidation–hydrogenation strategy for cleavage of C–C in lignin. By combination of C–O bond hydrogenolysis over Ru/CeO_2 catalyst and C_{aryl}–C_α bond oxidative cleavage, poplar lignin was converted into phenol[110]. **e** | C_{arom}–C_{arom} bond cleavage promoted by inserting a recyclable directing group[114]. The phenol moiety was used as a key handle to form a phosphinite-based group that enables Rh insertion and subsequent cleavage of the C_{arom}–C_{arom} bond. DCX, decarboxylation; PC, polycarbonate; PS, polystyrene. Part **c** adapted with permission from REF.[111], Elsevier.

the rate of hydrogenolysis of C_{arom}–C_{aliph} linkages may be required.

Oxidation–hydrogenation. The presence of water is beneficial for catalyst stability owing to the competitive adsorption of water and phenol enabling the removal of phenol from the ZSM-5 surface[109]. In contrast to the direct cleavage of the phenylpropanoid C_{arom}–C_{aliph} bond, Wang et al. proposed a stepwise cleavage of the C_{arom}–C_{aliph} bond via oxidative cleavage of the bond at the C_{α}–C_{β} position to acids and subsequent decarboxylation to break the C_{arom}–C_{aliph} bond[110] (FIG. 3d). Nonetheless, this strategy ignores the use of the abundant intrinsic propyl groups, which are potential sources to produce bio-based propylene.

Technologies for cleavage of C_{arom}–C_{arom}. C_{arom}–C_{arom} linkage is exceptionally strong, and therefore, breaking the C_{arom}–C_{arom} bond under harsh reaction condition would unavoidably induce unselective, deep-cracking of the reagent. Unlike the C–O, C=O and C–N bonds, C_{arom}–C_{arom} bonds are present in a nonpolar and unstrained form, leading to unmet adsorption on the catalyst surface[103,111–113]. Although the 5–5′ bond in biphenyls (FIG. 3a) can rotate freely to increase reactivity, substituent groups in lignin (for example, methoxy and alkyl groups) severely compromise the ability of the bond to rotate, hindering its accessibility to the catalyst. To our knowledge, only two approaches for the selective cleavage of the C_{arom}–C_{arom} bond in lignin have been demonstrated[103,114]. The first is to use the phenol moiety as a key handle to form a phosphinite-based group that enables Rh insertion and subsequent cleavage of the C_{arom}–C_{arom} bond[114] (FIG. 3e). In the second approach, the biphenyl unit in lignin first undergoes partial hydrogenation to transform the C_{arom}–C_{arom} bond into a more reactive C_{arom}–C_{aliph} bond, then follows the reductive cleavage mechanism to break the C_{arom}–C_{aliph} bond[103,111]. In addition, Weckhuysen and co-workers found that the 5–5′ bond is partially disrupted to form monomeric aromatic compounds during the cleavage of β–O–4 linkages over Pt/Al_2O_3 (REF.[115]).

To summarize, research on C_{arom}–C_{aliph} bond cleavage via cracking and hydrogenolysis in biomass over metal–metal oxide catalysts has intensified in recent years. Using a similar approach, it is possible to develop novel pathways to produce value-added chemicals from aromatic plastic. We highlight the following to consider during the development of new systems to break C_{arom}–C_{aliph} linkages in plastics. First, lignin is rich in oxygen, whereas plastics are not. Exploration on the influence of oxygen-containing groups to C_{arom}–C_{aliph} bond cleavage should be conducted. A recently reported CoS_2 catalyst enabled the cleavage of C_{arom}–C_{aliph} bonds in a lignin-derived oxygen-containing dimer, but is much less effective if oxygen is partially removed, highlighting the structure sensitivity[116]. Second, PF is abundant in hydroxy groups generating strong hydrogen-bonding networks. Breaking or tuning these hydrogen-bonding networks to increase its reactivity through designing functional ionic liquids and organic solvents, which has been well-studied in biomass conversion[117], is an interesting area for future research.

Conversion through ether bond cleavage

The ether bond is a major type of linkage in cellulose (β-1,4-glycosidic bond), lignin (e.g. 4–O–5, β–O–4, and α–O–4), and a range of oxygen-containing plastics such as epoxy resins (global production: 3.5 Mt yr^{-1})[118] and poly(*p*-phenylene oxide) (PPO, FIG. 4a, global production: 0.5 Mt yr^{-1})[119]. While glycosidic bonds should be regarded as a special acetal type ether bond, the nature of C–O bonds in lignin and ether-type plastics is similar. Indeed, all polyether plastics contain an ether-adjacent aromatic ring in their monomer, resembling the structure of lignin. The bond dissociation energy of ether bonds is normally less than C–C bonds (FIG. 4a), which is one reason that ether cleavage can be conducted under relatively low reaction temperatures. Hydrolytic, reductive, oxidative, and thermal depolymerization have all been adopted for the selective cleavage of the interunit ether linkages in lignin (β–O–4, 4–O–5 and α–O–4)[11]. Among these, reductive and oxidative methods have drawn immense attention.

Reductive cleavage using H_2. Reductive cleavage of the interunit ether linkages in lignin is usually catalysed by a metal or metal–acid catalyst (FIG. 4b). A wide variety of catalysts including noble (Ru, Rh, Pd and Pt) and non-noble (Ni, Cu, Fe and Co) metals has been investigated to generate aromatic products[120]. Research into the structure–activity relationship of the metal catalysts has presented some key findings. First, the inherent hydrogenation ability of noble metal is a key factor in the hydrodeoxygenation of lignin monomers. If the hydrogenation function is too strong (for example, Pt, Pd and Rh), it hydrogenates the aromatic ring; if too weak (for example, Cu), oxygen cannot be removed. Second, a strong interplay between metal nanoparticle size, charge state and product selectivity is often observed. Smaller metal particles with enhanced charge state restrain the co-adsorption of aromatic rings under planar configurations[121,122], which leads to higher selectivity towards aromatic products[123–125]. In the case of Ni catalysts, smaller Ni particles favour hydrodeoxygenation, whereas larger particles are more active in C–C hydrogenolysis[126]. More detailed discussions on the effect of particle size in biomass conversion is provided in a recent review[127]. Last, support and promoters often have an active role in regulating electronic and geometric properties of supported metal species. Use of a metal oxide support promotes C–O bond activation via the formation of covalent bonds along with strong chemisorption of oxygen-functional groups (for example, C–O and C=O). In this regard, oxophilic metal oxides showing Lewis acidity (for example, NbO_x, MoO_x, TiO_x, ReO_x, WO_x, TaO_x and VO_x) have received considerable attention[120,128]. After a decade of extensive research efforts, the selective catalytic cleavage of the interunit ether linkages in lignin, which was regarded as a challenging task in biomass utilization, was successfully achieved in many laboratories[129].

The reaction mechanism of the reductive cleavage of lignin depends on the type of ether unit and catalyst used[130]. β–O–4 and α–O–4 bonds can be cleaved by direct hydrogenolysis due to their lower bond

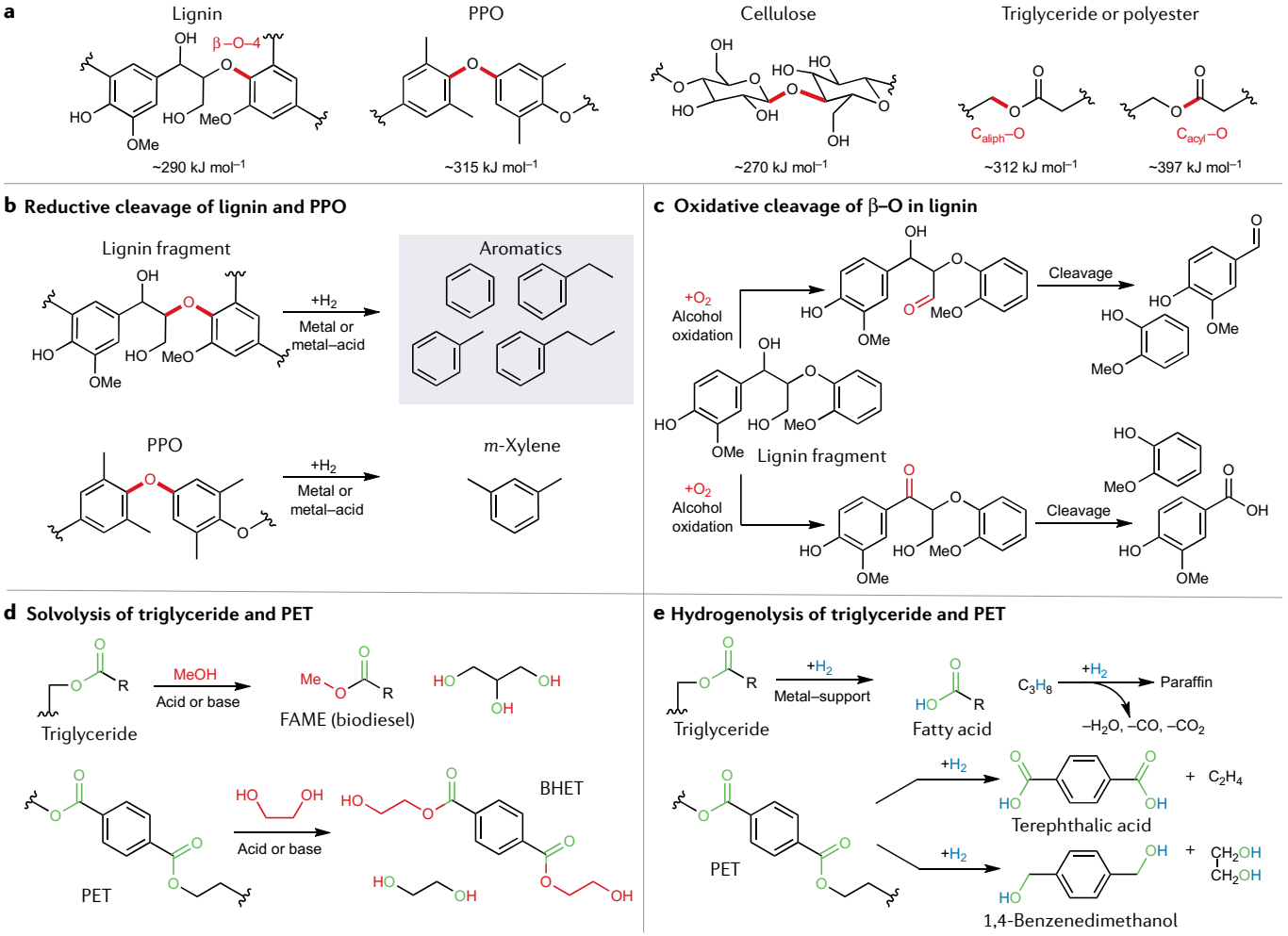

Fig. 4 | **Conversion strategies of C–O bond linkages in biomass valorization and plastic upcycling. a** | Bond dissociation energy of various C–O bonds in biomass and plastics. The bond dissociation energies were calculated with density functional theory. The details are described in the footnote † to FIG. 2. **b** | Reductive cleavage of the ether group in lignin and poly(*p*-phenylene oxide) (PPO). **c** | Oxidative cleavage of the β–O linkage in lignin. **d** | Solvolysis of triglyceride and polyethylene terephthalate (PET). Following a nucleophilic attack, C_{acyl}–O cleavage of the ester group occurs in both feeds. **e** | Hydrogenolysis of triglyceride and PET. Heterogeneous metal–support catalyst leads to C_{aliph}–O cleavage, thereby producing fatty acid plus propane from triglyceride. The hydrogenolysis pathway of PET depends on the type of catalyst. C_{aliph}–O cleavage occurs using heterogeneous C/MoO_2 (REF.[187]), whereas the homogeneous Ru catalyst[188,189] leads to C_{acyl}–O bond cleavage. BHET, bis(2-hydroxyethyl) terephthalate; FAME, fatty acid methyl ester.

dissociation energy, whereas the cleavage of the 4–O–5 bond occurs either by direct hydrogenolysis or by parallel hydrogenolysis–hydrolysis pathways. For example, the reductive cleavage of 4–O–5 linkages over supported Ni, Ru, Pt or Rh catalysts occurs via direct hydrogenolysis[131], but over Pd/C, the aromatic ether is first partially hydrogenated into an enol ether intermediate, which is highly susceptible to water attack to form a hemiacetal, before undergoing an elimination step to phenol/alkanol products and cyclohexanone[132].

Although the reductive depolymerization of polyether plastics is not studied extensively, the successful conversion of polyethers such as PPO has recently been demonstrated[104]. There are four possible pathways for the reductive depolymerization of PPO leading to different products depending on reaction conditions: (1) removal of oxygen and preservation of the benzene ring to produce *m*-xylene, (2) total hydrodeoxygenation to generate the corresponding cycloalkane, (3) selective ether cleavage to produce phenol, and (4) selective ether cleavage followed by hydrogenation to form ketones/alcohols. For the production of *m*-xylene (pathway 1), a combination of small, positively charged metal nanoparticle and weak acidic supports is required[104]. For the total hydrodeoxygenation of lignin to aromatics and cycloalkanes (pathway 2), in addition to the aid from acidic supports, metal components with high hydrogenation function (for example, Pd, Pt, Ru and Ni) are desirable[133–136]. For phenol production (pathway 3), the catalytic systems must be able to cleave the ether linkages while preserving the phenolic hydroxy groups. Therefore, using a metal component with poor hydrogenation performance (for example, Au and Ag) to allow for the retention of the phenolic hydroxy groups in lignin chemistry would be a beneficial strategy[137,138]. To favour the production of ketone/alcohol products (pathway 4), an additional arene hydrogenation function has to be incorporated using a proper metal element[131]. A clear difference between the cleavage of 4–O–5 linkages in lignin and the ether bonds in PPO, when targeting phenols as the product, is that the different position of C–O bond

cleavage in PPO will result in different phenolic products. That is, cleavage of the C–O bond having ortho-methyl substituted groups generates 3,5-dimethylphenol, whereas cleavage of the C–O bond having meta-methyl substituted groups affords 2,6-dimethylphenol, providing an opportunity for the selective production of 3,5-dimethylphenol or 2,6-dimethylphenol.

Reductive cleavage using other reagents. In addition to H_2 gas, other agents can also be used to produce aromatic products from diaryl ethers[139]. Various compounds such as amines or ammonia[130,140], organosilanes[141], $LiAlH_4$ (REF.[142]) and borohydrides[143] have been studied as potential reducing agents. Notably, reductive amination using amines or ammonia generates value-added N-containing chemicals for applications in pharmaceuticals, agrochemicals and other chemical industries[144,145]. Reductive amination is mostly investigated by using model compounds (for example, monomeric alcohols, aldehydes and carboxylic acids), whereas its effectiveness in transforming native lignin and real plastics into aniline derivatives remains to be demonstrated.

Conversely to thermocatalysis, electrocatalysis can be operated under milder reaction conditions. Variation of cell potential offers a more delicate control of product distribution, potentially leading to higher selectivity. Among various biomass and plastic feeds, electrocatalytic approaches have been reported almost exclusively for ether-containing feeds such as lignin, model ether-linked compounds and cellulose[30,143,146–150]. This is presumably because the ether bond has the weakest bond energy among linkages (FIGS. 2a,3a and 4a), and ether-containing feeds are more soluble in electrolyte solutions, which are typically acidic or basic solutions, than others. As such, electrocatalytic reduction of three types of ether bonds (α–O–4, β–O–4 and 4–O–5) was realized at room temperature and atmospheric pressure in air using an undivided cell with two electrodes system[143]. Lercher and co-workers mentioned that thermal and electrochemical routes share the 'same reaction pathways' during conversion of phenols and diaryl ethers[150]. They suggested that the reaction rates of electrocatalytic hydrogenation are positively associated with negative potentials, which is related to the coverage of adsorbed hydrogen on the catalyst surface[150]. As with thermocatalytic hydrogenolysis, several metal (for example, Pt, Pd, Ru, Rh and Pd) supported carbon catalysts were reported as efficient catalysts for ether cleavage of lignin monomers[30,147,149]. Among them, Pd/C showed inactiveness to aromatic ring hydrogenation unlike Pt/C and Rh/C during electrocatalytic phenol hydrogenation[149]. As breaking C–O bonds while preserving the benzene ring is critical[30,147], Pd is more promising than other elements in the electrocatalytic reduction of lignin. Although not proven, the similarity of bond activation chemistry between thermocatalysis of lignin and PPO suggests that electrocatalysis can be a feasible technology for upcycling polyether plastics too.

Oxidative cleavage. Oxidative cleavage is a unique pathway, which is currently almost exclusively practiced in lignin conversion (FIG. 4c). This transformation breaks β–O–4 bonds via a radical mechanism, but does not work well with other C–O/C–C linkages, such as 4–O–5, 5–5′ and so on[110,151]. The pre-oxidation of the α-hydroxyl groups to the α-carbonyl groups is beneficial because it allows for further reaction, as it decreases the dissociation energy of the C_β–O bond (from 248 to 161 kJ mol^{-1})[129] to allow its cleavage under mild conditions[129,152,153]. A disadvantage of the pathway is the special structural requirement of substrate: the oxidation of side-chain linkages and phenolic hydroxyl groups needs the presence of hydroxyl groups. Even for the aromatic rings in lignin, the oxidation reaction only occurs on substituted phenols[154]. Photocatalysis of the β–O–4 bond is another example of oxidative cleavage. Two strategies, based on stepwise conversion and direct cleavage, have been developed[12]. The stepwise pathway begins with the pre-oxidation of the α-hydroxy groups to α-carbonyl groups, then the C_β–O bond is cleaved with the aid of photo-derived electrons. The direct photocatalytic cleavage of the C_β–O bond proceeds through a redox-neutral manner and avoids the consumption of reductants and oxidants associated with the stepwise pathway.

Hydrolysis of the glycosidic bond. The glycosidic bond is a special type of bond that exists in biomass such as cellulose and chitin, and is susceptible to hydrolysis. Hydrolysis over a strong mineral acid (for example, HCl) allows nearly 100% conversion into monomers, but the process suffers from the heavy use of corrosive reagents, harsh reaction conditions and the generation of unwanted products. In recent years, recyclable and environmentally benign chemical catalytic systems using various solid acids such as Amberlyst[155], sulfonated carbon[156,157], oxidized carbon[158], zeolites[159] and heterogenized polyoxometalates (that is, polyoxometalates transformed to insoluble solids by ion exchange or immobilized on the solid support)[160] have been established. Swelling of the dense cellulose domain to a loosely packed structure alleviates the secondary interaction, making hydrolysis more efficient. The use of co-solvent systems that partially swell the cellulose[161–164] or chitin[165] chain have also been reported.

Clearly, ether bond cleavage is intensively studied through lignin and cellulose conversion. Although not every system identified for biomass feedstock is directly transferable to convert waste polyether plastics due to the special structural requirement in certain conversions, inspirations for upcycling of polyethers such as PPO could indeed be drawn from research in lignin depolymerization. A key challenge is to identify a catalyst that enables the selective activation of one of the bilateral C–O bonds in ether linkages in polyethers. In addition, theoretical and experimental analyses on reaction mechanism should be conducted to understand the influence of monomer structure, such as the position of alkyl/alkoxy substituents, on reactivity.

Conversion through ester bond cleavage

The ester bond is a linking unit in triglyceride as well as in several polyester and PC plastics, such as PET (global production of 38 Mt per year)[20] and PC, that are widely found in bottle, film, fibre and electronic devices. Ester

compounds contain two different C–O bonds: C_{aliph}–O and C_{acyl}–O bonds. In aliphatic esters, the bond dissociation energy of C_{acyl}–O is about 80–90 kJ mol^{-1} higher than that of C_{aliph}–O (FIG. 4a), whereas in phenyl benzoate, the strength of C_{aliph}–O is more than 110 kJ mol^{-1} higher than C_{acyl}–O[166]. These imply that the bond dissociation energy of C–O vary enormously depending on the adjacent substituents.

Solvolysis. Esters are formed via condensation of alcohols and carboxylic acids, thus are prone to be cleaved following nucleophilic attack. Various nucleophilic reagents have been evaluated to break down the ester linkage. As these reagents are normally used in large excess and also act as the reaction solvent, this process is conventionally called solvolysis (FIG. 4d). Solvolysis of polyesters leads to high conversion into the constituent monomers, and therefore has attracted substantial industrial interest. In parallel, transesterification of triglyceride is one of the most practiced biomass utilization technologies. By using a simple alcohol (methanol or ethanol) in the presence of inorganic basic (for example, NaOH and KOH) or acidic (for example, H_2SO_4 and HCl) catalysts, biodiesel (fatty acid methyl or ethyl ester) can be generated in quantitative yield[167,168].

In waste plastic recycling, glycolysis — solvolysis using an ethylene glycol solvent — is a mature process used to treat PET to recover the bis(2-hydroxyethyl) terephthalate (BHET) monomer. Not only strong acids and bases but also various metal halides and acetates (for example, zinc acetate) are identified as effective catalysts for this transformation. Glycolysis does not require complex separation steps because the by-product, ethylene glycol, is another monomer of PET, enabling circular process of plastic synthesis from waste plastic (depolymerization–repolymerization). Other substances such as methanol, ethanol, ammonia, amines and water can also be used as reagents[169,170]. Solvolysis is mostly conducted in homogeneous solution phase, therefore fast mass/heat transfer is critical. Various strategies such as adopting ionic liquids as catalysts[161–174], using microwave-assisted heating[175,176], using a supercritical solvent[170,177,178] and conducting ultrasound-assisted reactions[179,180] have been vividly explored to enhance process efficiency. Owing to its simple process design and environmental benefits from reduced waste emissions, solvolysis has been widely adopted to recycle PET by chemical companies such as BP Infinia, Dupont Teijin Films and Eastman[181,182]. Research interests of solvolysis are not limited to thermocatalysis. Recently, Zhou et al. showed a successful electrocatalytic hydrolysis of waste PET to produce commodity chemicals (potassium diformate and teretphthalic acid paired with H_2) with >80% Faradaic efficiency by using a $CoNi_{0.2}$5P catalyst and aqueous KOH electrolyte[183]. Solvolysis has also been adopted to treat a range of polyesters[184] and PCs[172,179] to recover their constituent monomers.

Hydrogenolysis. Hydrogenolysis is another powerful strategy to break ester linkages (FIG. 4e). Without a catalyst, thermal degradation of ester-type polymers results in the cleavage of C_{aliph}–O bonds, with β-elimination as the major pathway. H_2 treatment using a metal catalyst allows for a decreased reaction temperature and fine control of the degree of reduction, thus enabling diverse products such as carboxylic acids (plus alkanes), and subsequently aldehydes, alcohols and alkanes via sequential reduction[185,186]. Recent work by Kratish et al.[187] reveals the specific roles of heterogeneous catalysts in the hydrogenolysis of polyester compounds such as PET[187]. On the basis of a study using a C/MoO_2 catalyst, it was suggested that β-elimination is accelerated by bidentate adsorption of the ester substrate on the low-coordinate MoO_x site followed by a nucleophilic attack of activated hydrogen to the carbonyl group, after which PET was deconstructed into terephthalic acid and ethylene in 80 wt% yield (FIG. 4e). Coversely, Krall et al. reported that Ru(II) PNN pincer catalysts transformed a range of polyesters into diols and PCs into glycols and methanol in >80 wt% conversion[188]. The fact that diols and methanol were produced instead of carboxylic acids and hydrocarbons suggests that the depolymerization took place in the C_{acyl}–O bond. Only poly(R-3-hydroxybutyric acid) (PHB) and poly(3-hydroxypropionic acid) (P3HP) were exceptional cases in which carboxylic acid plus hydrocarbons were still the favoured product. Similar results were also reported in another study using molecular Ru catalysts such as [Ru(triphos)tmm] or [Ru(triphos-xyl)tmm] (REF.[189]). Encouragingly, even commercial plastic sources (for example, water bottles, yoghurt pots, and so on) were transformed to their monomeric diols at nearly 100% conversion and selectivity[189]. As mentioned in the earlier section, hydroconversion of triglycerides produces hydrocarbons because of the fast deoxygenation, in particular at high levels of conversion, whereas the current commercial routes to produce fatty alcohols from natural lipids involve multiple transesterification steps[190]. In this regard, new catalytic systems capable of promoting the C_{acyl}–O bond cleavage, as demonstrated in PET upcycling, would unlock a new conversion route of triglyceride to co-produce fatty alcohols and glycerol in a single step. Moreover, the catalytic system for the chemoselective C–O bond cleavage may be extended to downstream processes in biomass refineries, such as pyrolysis oil upgrading if alcohols are the desired products over hydrocarbons.

In all, solvolysis is a well-developed strategy to break the ester linkage in triglycerides and polyesters, although different nucleophilic reagents are used for each substrate. Reductive cleavage of the ester bond in plastic waste has recently been explored. Heterogeneous and homogeneous catalysts can lead to distinct selectivity differences in bond cleavage. Although triglyceride hydroconversion is successfully operating on a commercial scale, development of chemoselective catalytic systems will open up more transformation opportunities for the conversion of ester-containing biomass and plastics.

Conversion through C–N bond cleavage

Amides are an important linkage in proteins, certain plastics and chitin. Proteins are a class of natural functional biopolymers linked together by condensation of amine and carboxylic acid groups of various amino acids.

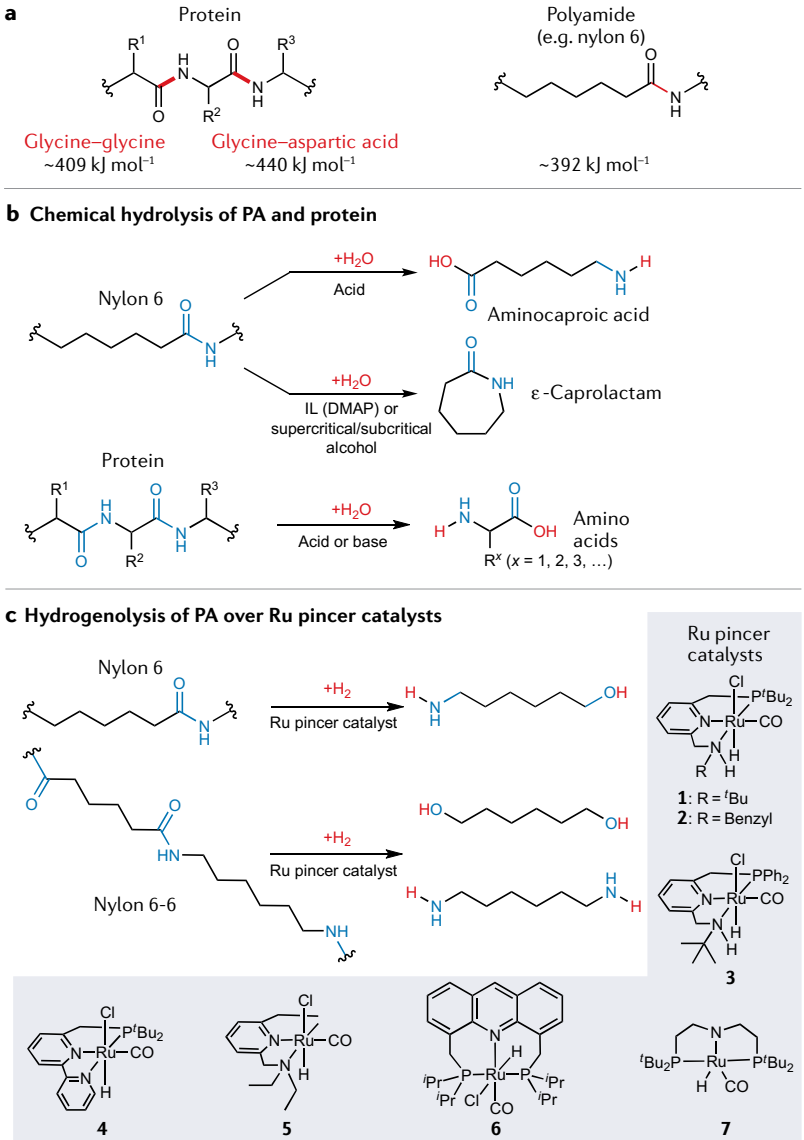

Fig. 5 | **Conversion strategies of C–N linkages in biomass valorization and plastic upcycling. a** | Bond dissociation energy of various C–N bonds in biomass and plastics. The bond dissociation energies were calculated with density functional theory. The details are described in the footnote † to FIG. 2. **b** | Chemical hydrolysis of polyamide (PA) and protein. PA can be cleaved in various ways depending on the reagent and catalyst. **c** | Hydrogenolysis of PA using Ru pincer catalysts[213]. It is used to upcycle waste PA into aminoalcohol or the pair of diol and diamine. DMAP, N,N-dimethylpyridin-4-amine.

Presently, amino acids are used as food additives, in cosmetics and in pharmaceutical products, all having production capacities that are constantly increasing[191]. In the plastic domain, synthetic polyamides (PAs) are widely applied in the textile manufacturing and automotive industries due to its superior durability and strength (global production of PA-6 and PA-6,6 (that is, nylon 6 and nylon 6–6; FIG. 5) of 9 Mt per year)[192]. Another important plastic containing a C–N bond is polyurethane (global production of 24 Mt per year)[193]. Amides also exist in the side chain of chitin, but it is preferential that these linkages are preserved rather than cleaved to valorize chitin into N-containing chemicals[194,195]. Amides show more pronounced chemical inertness than carboxylic acids and other carbonyl derivatives because of the decreased electrophilicity of their carbonyl groups, derived from resonance effects[196]. The bond dissociation energy of an amide bond in typical proteins and PAs reaches ~400 kJ mol^{-1} (FIG. 5a).

Solvolysis. Like the ester linkage, the amide bond can be cleaved through solvolysis in organic solvents and in aqueous phase (hydrolysis). Hydrolysis of PA-6 (that is, nylon 6 or polycaprolactam) and hydroglycolysis of polyurethane has reached commercialization stage. Interestingly, in the glycolysis of PA-6,6 (that is, nylon 6-6), the major products were diamine plus aliphatic ester compounds, as well as cyclic δ-valerolactone[197], suggesting that the solvolysis of PAs has a more complex reaction pathway than that of polyesters and PCs. The product distribution is sensitive to the reaction media and conditions. For instance, aliphatic PAs are depolymerized to aliphatic aminocaproic acid under a mineral acid catalyst during hydrolysis[198–200], whereas when running the reaction under supercritical secondary alcohol media or with an ionic liquid catalyst, it greatly increases the selectivity of cyclic monomers[201,202] (FIG. 5b). The factors governing product selectivity are still under investigation. One observation is that solvents with less sterically hindered nucleophilic atoms (for example, water and primary alcohols) induce intermolecular depolymerization between the solvent and the PA, leading to aliphatic monomer products. By contrast, the solvents with large steric hindrance (for example, secondary and tertiary alcohols) induce an intramolecular reaction of the PA, leading to cyclic monomer products[202]. Proteins can be depolymerized into amino acids via chemical hydrolysis in the presence of strong acids or base (FIG. 5b). Before 1950, it was the primary method to manufacture amino acids; however, chemical hydrolysis has some critical drawbacks, including waste generation, reactor corrosion, risk of leakage and product decomposition[203,204]. Thus, it is no longer conducted on a large scale.

Hydrogenolysis. There have been major developments in the use of homogeneous catalysts for C–N cleavage using H_2 in the past two decades[196]. Most systems used short-chain amides as a model substrate for identifying the active catalyst. Diverse Ru pincer complexes (for example, PN, NN and PNN types: P and N indicate the chelating atoms of the ligand)[205–207] as well as Fe-centred[208] and Mn-centred pincer complexes[209] were introduced as active C–N cleavage catalysts. In the domain of heterogeneous catalysis, several examples exhibited good selectivity towards C–N bond cleavage, although the majority of catalysts showed higher C–O bond cleavage selectivity than the C–N bond. In a recent report, an Ag/γ-Al_2O_3 catalyst combined with a potassium *tert*-butoxide (KO*t*Bu) promoter was capable of hydrogenating secondary amides (selectivity ~100%)[210]. Tomishige and co-workers reported CeO_2 supported a Ru catalyst for the C–N cleavage of primary amide in water with >90% selectivity[211]. In another study, a Pd/In_2O_3 catalyst was remarkably effective in breaking primary, secondary and tertiary amides while preventing hydrogenation of aromatic side chains[212]. Very recently, Milstein's group

Table 1 | **Summary of catalytic conversion of various plastic and biomass substrates via activating C–C, C–O and C–N bonds**

Bonds		Feedstocks	Methods	Catalysts	Products
C–C	C_{aliph}–C_{aliph}	Ubiquitous in biomass and plastic	Catalytic cracking	Brønsted acid	Paraffins, light olefins and bio-oils
			Hydrogenolysis	Metal	Paraffins and aromatics
			Hydrocracking	Metal–acid	*iso*-Paraffins
			Metathesis (requiring C=C bond)	Homogeneous and heterogeneous metathesis catalysts	Hydrocarbons
			Retro-aldol reaction (requiring β-hydroxy carbonyl unit)	Metal–Lewis acid	Polyols and alcohols
	C_{arom}–C_{aliph}	Lignin fragments featuring β–5, β–1, β–β and α–1 linkages, PS, PC and PF	Catalytic cracking	Brønsted acid	Aromatics and phenolics
			Reductive cleavage	Metal and metal–acid	Aromatics, cycloalkanes and phenolics
			Oxidation–hydrogenation (requiring β-O–4 linkages)	Combination of metal and oxidant	Phenol
	C_{arom}–C_{arom}	Lignin fragments featuring 5-5′ linkages	Reductive cleavage	Homogeneous and heterogeneous metal catalysts, and metal–acid	Phenolics
					Aromatics and cycloalkanes
C–O	Ether bond	Cellulose, chitin, lignin, epoxy resins and PPO	Reductive cleavage using H_2	Metal and metal–acid	Phenolics, aromatics and cycloalkanes
			Reductive cleavage using other reagents (for example, amine, organosilane and $LiAlH_4$)	Metal	Phenolics and N-containing chemicals
			Oxidative	Acid, base and metal–organic	Aromatic oxygenated chemicals
			Hydrolysis (requiring a glycosidic bond)	Metal halides and acid	Carbohydrates
	Ester bond	Triglyceride, PET and PC	Solvolysis	Acid, base, metal halides and acetates	Alcohol and carboxylic acids
			Hydrogenolysis	Metal and metal–acid	Alcohol, carboxylic acids and hydrocarbons
C–N	Amide bond	Protein, PA and PU	Solvolysis	Strong acid, strong base and transition metal salts	Amino acids and aliphatic ester/ aminocaproic acid
			Hydrogenolysis	Metal and metal-centred pincer catalysts	Amides, amino alcohols and polyols

PA, polyamide; PC, polycarbonate; PET, polyethylene terephthalate; PPO, poly(*p*-phenylene oxide); PU, polyurethane.

demonstrated the first example of plastic depolymerization via reductive C–N bond cleavage using Ru PNN and PNP complexes[213] (FIG. 5c). Various PAs such as nylon 6, nylon 6-6 and nylon 12 were transformed to corresponding monomeric and oligomeric amino alcohols (or diol plus diamine) with ≥60% conversion. Although the system requires harsh reaction conditions (150 °C, 70 bar of H_2 and KO*t*Bu in DMSO as a co-catalyst), it paves a way for selective degradation of PA via an unconventional C–N cleavage pathway.

In short, solvolysis is applicable to the depolymerizion of both PAs and proteins, but ecofriendly and efficient chemical catalysts remain a challenge, particularly for protein feedstocks. In the future, non-toxic, recyclable heterogeneous catalytic systems may be developed for both PA and protein hydrolysis/solvolysis. Meanwhile, the concept of reductive depolymerization of PAs has been proposed and developed. The major research interest has been achieving selective cleavage of C–N bonds over C–O and C–C bonds. Only homogeneous catalytic

systems are proven to be effective catalysts for the conversion of real plastic feedstocks at present. The conversion of biomass and plastics through C–N cleavage is still in the early stage of development, with many opportunities remaining for future research and development.

Conclusions and perspectives

To harness the full potential of biomass and plastics as organic carbon feedstocks, it is of prime importance in future investigations to explore environmentally benign and economically viable transformation processes. By comparing the catalytic transformation of biomass and plastic waste through a unified angle, it is apparent that many strategies are applicable for both feedstocks. Although thermal processes (that is, gasification and pyrolysis) are already practiced at the commercial level, catalytic strategies can improve the present process efficiency and unlock new transformation pathways. Emerging catalytic strategies for the activation of C–C, C–O and C–N bonds in biomass and plastics share common features. These catalytic systems are broadly divided into reductive, oxidative and neutral pathways regardless of feedstock, and in each category, there exist general mechanisms for catalytic function and catalyst design principles (TABLE 1). The reaction and catalyst design principles can also be transferred to emerging technologies such as electrocatalysis and photocatalysis.

Through the 'unified view' in this Review, we identified which scientific challenges have been relatively well tackled, and those that are underexplored or remain to be addressed. As such, future research directions can be suggested with the following concept: for areas in which biomass valorization has been extensively developed, ample opportunities exist for waste plastic upcycling by adopting similar approaches, and vice versa. The cleavage of a typical C_{aliph}–C bond in biomass and plastics already makes extensive use of experience obtained from petroleum refineries. Cleavage of oxygen-linked C–C bonds, which are majorly developed in biomass, hints at new depolymerization strategies of plastics containing polar elements such as PVC. Even in the case of the inert C_{aliph}–C bond, there is the possibility of new strategies such as oxidation-assisted depolymerization. Numerous insights gained from the lignocellulose conversion on C_{arom}–C and ether cleavage can be harnessed into the upcycling of plastics, especially to produce aromatic monomers. For the rather weak ether linkage in biomass, successful demonstrations of electrocatalysis and photocatalysis have been reported recently, inspiring the potential of these strategies for ether-linked plastics. The conversion of triglyceride and polyester through ester cleavage has common features in terms of reaction pathway and type of catalysts. Nevertheless, the recent appearance of bond cleavage selectivity (C_{acyl}–O versus C_{aliph}–O) in the polyester hydrogenolysis can facilitate novel applications of triglyceride conversion.

In the future, the identification of catalytic active sites and improved understanding of reaction mechanism is essential. For hydrogenation, the relative activity of C–C scission, C–O/N scission and C=C saturation of numerous active metal components, such as Cu, Ni, Pd, Pt, Ru, and so on, remains an interesting topic. Microkinetic modelling and quantitative structure–activity relationships would have a profound effect on catalyst design. There are also substantial differences in the compositional and molecular size gaps between the two feedstocks. Furthermore, the rigid polymer framework structure of biomass and plastics arising from intramolecular interactions leads to poor contact between polymers and catalytic active sites. Thus, special attention beyond bond activation should be paid to enhance the accessibility of polymer substrates to catalytic active sites. Another challenge is the handling of impurities. Raw biomass and waste plastic feeds are generally composite materials, not only with polymers but also with other inorganic substances. Although the separation and purification processes precede any chemical conversions, in most cases impurities such as alkali metals, sulfur, halogens and heavy metals can remain in the substrate. Combined, a range of issues including pretreatment, melting/solubilization, purification of the feedstock and reactor engineering must be addressed, together with extensive catalyst development, to implement valorization/upcycling of biomass and plastics via catalytic processes.

Published online 11 August 2022

1. International Energy Agency. Technology roadmap: delivering sustainable bioenergy (IEA, 2017).
2. Malico, I., Nepomuceno Pereira, R., Gonçalves, A. C. & Sousa, A. M. O. Current status and future perspectives for energy production from solid biomass in the European industry. *Renew. Sustain. Energy Rev.* **112**, 960–977 (2019).
3. National Renewable Energy Laboratory. *Chemicals from Biomass: a Market Assessment of Bioproducts with Near-term Potential* (NREL, 2016); https://www.nrel.gov/docs/fy16osti/65509.pdf
4. Garcia, J. M. & Robertson, M. L. The future of plastics recycling. *Science* **358**, 870–872 (2017).
5. Zheng, J. & Suh, S. Strategies to reduce the global carbon footprint of plastics. *Nat. Clim. Change* **9**, 374–378 (2019).
6. Geyer, R., Jambeck, J. R. & Law, K. L. Production, use, and fate of all plastics ever made. *Sci. Adv.* **3**, e1700782 (2017).
7. Adyel, T. M. Accumulation of plastic waste during COVID-19. *Science* **369**, 1314–1315 (2020).
8. Ritter, S. K. Lignocellulose: a complex biomaterial. *Plant Biochem.* **86**, 15 (2008).
9. Sun, Z., Fridrich, B., de Santi, A., Elangovan, S. & Barta, K. Bright side of lignin depolymerization: toward new platform chemicals. *Chem. Rev.* **118**, 614–678 (2018).
10. Sudarsanam, P., Peeters, E., Makshina, E. V., Parvulescu, V. I. & Sels, B. F. Advances in porous and nanoscale catalysts for viable biomass conversion. *Chem. Soc. Rev.* **48**, 2366–2421 (2019).
11. Schutyser, W. et al. Chemicals from lignin: an interplay of lignocellulose fractionation, depolymerisation, and upgrading. *Chem. Soc. Rev.* **47**, 852–908 (2018).
12. Wu, X. et al. Photocatalytic transformations of lignocellulosic biomass into chemicals. *Chem. Soc. Rev.* **49**, 6198–6223 (2020).
13. Shrotri, A., Kobayashi, H. & Fukuoka, A. Cellulose depolymerization over heterogeneous catalysts. *Acc. Chem. Res.* **51**, 761–768 (2018).
14. Granone, L. I., Sieland, F., Zheng, N., Dillert, R. & Bahnemann, D. W. Photocatalytic conversion of biomass into valuable products: a meaningful approach? *Green Chem.* **20**, 1169–1192 (2018).
15. Liu, X., Duan, X., Wei, W., Wang, S. & Ni, B.-J. Photocatalytic conversion of lignocellulosic biomass to valuable products. *Green Chem.* **21**, 4266–4289 (2019).
16. Yoo, C. G., Meng, X., Pu, Y. & Ragauskas, A. J. The critical role of lignin in lignocellulosic biomass conversion and recent pretreatment strategies: a comprehensive review. *Bioresour. Technol.* **301**, 122784 (2020).
17. Rahimi, A. & Garcīa, J. M. Chemical recycling of waste plastics for new materials production. *Nat. Rev. Chem.* **1**, 0046 (2017).
18. Coates, G. W. & Getzler, Y. D. Y. L. Chemical recycling to monomer for an ideal, circular polymer economy. *Nat. Rev. Mater.* **5**, 501–516 (2020).
19. Vollmer, I. et al. Beyond mechanical recycling: giving new life to plastic waste. *Angew. Chem. Int. Ed.* **59**, 15402–15423 (2020).
20. Martín, A. J., Mondelli, C., Jaydev, S. D. & Pérez-Ramírez, J. Catalytic processing of plastic waste on the rise. *Chem* **7**, 1487–1533 (2021).
21. Zhang, X., Fevre, M., Jones, G. O. & Waymouth, R. M. Catalysis as an enabling science for sustainable polymers. *Chem. Rev.* **118**, 839–885 (2018).
22. Sohn, Y. J. et al. Recent advances in sustainable plastic upcycling and biopolymers. *Biotechnol. J.* **15**, e1900489 (2020).
23. Huber, G. W., Iborra, S. & Corma, A. Synthesis of transportation fuels from biomass chemistry, catalysts, and engineering. *Chem. Rev.* **106**, 4044–4098 (2006).

24. Al-Salem, S. M., Lettieri, P. & Baeyens, J. Recycling and recovery routes of plastic solid waste (PSW): a review. *Waste Manag.* **29**, 2625–2643 (2009).
25. Ragaert, K., Delva, L. & Van Geem, K. Mechanical and chemical recycling of solid plastic waste. *Waste Manag.* **69**, 24–58 (2017).
26. Zhou, C. H., Xia, X., Lin, C. X., Tong, D. S. & Beltramini, J. Catalytic conversion of lignocellulosic biomass to fine chemicals and fuels. *Chem. Soc. Rev.* **40**, 5588–5617 (2011).
27. Ennaert, T. et al. Potential and challenges of zeolite chemistry in the catalytic conversion of biomass. *Chem. Soc. Rev.* **45**, 584–611 (2016).
28. Miandad, R., Barakat, M. A., Aburiazaiza, A. S., Rehan, M. & Nizami, A. S. Catalytic pyrolysis of plastic waste: a review. *Process. Saf. Environ. Prot.* **102**, 822–838 (2016).
29. Nikles, D. E. & Farahat, M. S. New motivation for the depolymerization products derived from poly(ethylene terephthalate) (PET) waste: a review. *Macromol. Mater. Eng.* **290**, 13–30 (2005).
30. Garedew, M. et al. Electrochemical upgrading of depolymerized lignin: a review of model compound studies. *Green Chem.* **23**, 2868–2899 (2021).
31. Chen, C.-C., Dai, L., Ma, L. & Guo, R.-T. Enzymatic degradation of plant biomass and synthetic polymers. *Nat. Rev. Chem.* **4**, 114–126 (2020).
32. Marignan, A.-L. Anellotech's Bio-TCat™ technology for making Bio *p*-xylene, toluene and benzene from woody biomass is ready for commercialization. *IFP Energies Nouvelles* https://www.ifpenergiesnouvelles.com/article/anellotechs-bio-tcattm-technology-ready-commercialization (2021).
33. Marker, T. L., Felix, L. G., Linck, M. B. & Roberts, M. J. Integrated hydropyrolysis and hydroconversion (IH^2) for the direct production of gasoline and diesel fuels or blending components from biomass, part 1: proof of principle testing. *Environ. Prog. Sustain. Energy* **31**, 191–199 (2012).
34. Vásquez, M. C., Silva, E. E. & Castillo, E. F. Hydrotreatment of vegetable oils: a review of the technologies and its developments for jet biofuel production. *Biomass Bioenergy* **105**, 197–206 (2017).
35. Baldiraghi, F. et al. in *Sustainable Industrial Chemistry* (eds Cabani, F., Centi, G., Perathoner, S. & Trifirò, F.) 427–438 (Wiley-VCH, 2009).
36. Weitkamp, J. Catalytic hydrocracking — mechanisms and versatility of the process. *ChemCatChem* **4**, 292–306 (2012).
37. Corma, A. & Orchillés, A. V. Current views on the mechanism of catalytic cracking. *Micropor. Mesopor. Mater.* **35–36**, 21–30 (2000).
38. Haag, W. & Dessau, R. Duality of mechanism for acid-catalyzed paraffin cracking. In *Proc. 8th International Congress on Catalysis* **2**, 305–316 (Dechema, 1984).
39. Vogt, E. T. & Weckhuysen, B. M. Fluid catalytic cracking: recent developments on the grand old lady of zeolite catalysis. *Chem. Soc. Rev.* **44**, 7342–7370 (2015).
40. Marker, T. L. *Opportunities for Biorenewables in Oil Refineries* (UOP, 2005); https://www.osti.gov/servlets/purl/861458
41. Williams, P. T. & Horne, P. A. Characterisation of oils from the fluidised bed pyrolysis of biomass with zeolite catalyst upgrading. *Biomass Bioenergy* **7**, 223–236 (1994).
42. Horne, P. A. & Williams, P. T. The effect of zeolite ZSM-5 catalyst deactivation during the upgrading of biomass-derived pyrolysis vapours. *J. Anal. Appl. Pyrolysis* **34**, 65–85 (1995).
43. Thring, R. W., Katikaneni, S. P. & Bakhshi, N. N. The production of gasoline range hydrocarbons from Alcell® lignin using HZSM-5 catalyst. *Fuel Process. Technol.* **62**, 17–30 (2000).
44. Huber, G. W. & Corma, A. Synergies between bio-and oil refineries for the production of fuels from biomass. *Angew. Chem. Int. Ed.* **46**, 7184–7201 (2007).
45. Corma, A., Huber, G., Sauvanaud, L. & O'Connor, P. Processing biomass-derived oxygenates in the oil refinery: catalytic cracking (FCC) reaction pathways and role of catalyst. *J. Catal.* **247**, 307–327 (2007).
46. Vollmer, I., Jenks, M. J. F., Mayorga Gonzalez, R., Meirer, F. & Weckhuysen, B. M. Plastic waste conversion over a refinery waste catalyst. *Angew. Chem. Int. Ed.* **60**, 16101–16108 (2021).
47. Tukker, A., de Groot, H., Simons, L. & Wiegersma, S. Chemical recycling of plastics waste (PVC and other resins) (TNO Institute of Strategy, Technology and Policy, Netherlands Organization for Applied Scientific Research (TNO), 1999).
48. Rorrer, J. E., Beckham, G. T. & Román-Leshkov, Y. Conversion of polyolefin waste to liquid alkanes with Ru-based catalysts under mild conditions. *JACS Au* **1**, 8–12 (2020).
49. Celik, G. et al. Upcycling single-use polyethylene into high-quality liquid products. *ACS Cent. Sci.* **5**, 1795–1803 (2019).
50. Tennakoon, A. et al. Catalytic upcycling of high-density polyethylene via a processive mechanism. *Nat. Catal.* **3**, 893–901 (2020).
51. Zhang, F. et al. Polyethylene upcycling to long-chain alkylaromatics by tandem hydrogenolysis/aromatization. *Science* **370**, 437–441 (2020).
52. Sotelo-Boyás, R., Trejo-Zárraga, F. & Hernández-Loyo, F. D. J. Hydroconversion of triglycerides into green liquid fuels. *Hydrogenation* **338**, 187–216 (2012).
53. Anderson, A. D., Lanci, M. P., Buchanan, J. S., Dumesic, J. A. & Huber, G. W. The hydrodeoxygenation of glycerol over NiMoSx: catalyst stability and activity at hydropyrolysis conditions. *ChemCatChem* **13**, 425–437 (2021).
54. Kim, M. Y., Kim, J.-K., Lee, M.-E., Lee, S. & Choi, M. Maximizing biojet fuel production from triglyceride: importance of the hydrocracking catalyst and separate deoxygenation/hydrocracking steps. *ACS Catal.* **7**, 6256–6267 (2017).
55. McCall, M. J., Kocal, J. A., Bhattacharyya, A., Kalnes, T. N. & Brandvold, T. A. Production of aviation fuel from renewable feedstocks. US patent US 8,039,682 B2 (2011).
56. Simley, J. Honeywell introduces simplified technology to produce renewable diesel. *Honeywell UOP* https://uop.honeywell.com/en/news-events/2021/january/honeywell-uop-ecofining-single-stage-process (2021).
57. Lee, K., Lee, M.-E., Kim, J.-K., Shin, B. & Choi, M. Single-step hydroconversion of triglycerides into biojet fuel using CO-tolerant PtRe catalyst supported on USY. *J. Catal.* **379**, 180–190 (2019).
58. Guisnet, M. "Ideal" bifunctional catalysis over Pt-acid zeolites. *Catal. Today* **218–219**, 123–134 (2013).
59. Alvarez, F., Ribeiro, F., Perot, G., Thomazeau, Y. C. & Guisnet, M. Hydroisomerization and hydrocracking of alkanes: 7. Influence of the balance between acid and hydrogenating functions on the transformation of *n*-decane on PtHY catalysts. *J. Catal.* **162**, 179–189 (1996).
60. Munir, D., Irfan, M. F. & Usman, M. R. Hydrocracking of virgin and waste plastics: a detailed review. *Renew. Sustain. Energy Rev.* **90**, 490–515 (2018).
61. Ding, W., Liang, J. & Anderson, L. L. Hydrocracking and hydroisomerization of high-density polyethylene and waste plastic over zeolite and silica-alumina-supported Ni and Ni-Mo sulfides. *Energy Fuels* **11**, 1219–1224 (1997).
62. Venkatesh, K. R. et al. Hydrocracking and hydroisomerization of long-chain alkanes and polyolefins over metal-promoted anion-modified zirconium oxides. *Energy Fuels* **10**, 1163–1170 (1996).
63. Joo, H. K. & Curtis, C. W. Catalytic coprocessing of LDPE with coal and petroleum resid using different catalysts. *Fuel Process. Technol.* **53**, 197–214 (1998).
64. Bin Jumah, A., Anbumuthu, V., Tedstone, A. A. & Garforth, A. A. Catalyzing the hydrocracking of low density polyethylene. *Ind. Eng. Chem. Res.* **58**, 20601–20609 (2019).
65. Liu, S., Kots, P. A., Vance, B. C., Danielson, A. & Vlachos, D. G. Plastic waste to fuels by hydrocracking at mild conditions. *Sci. Adv.* **7**, eabf8283 (2021).
66. Akah, A., Hernandez-Martinez, J., Rallan, C. & Garforth, A. Enhanced feedstock recycling of post-consumer plastic. *Chem. Eng. Trans.* **43**, 2395–2400 (2015).
67. Serrano, D. P., Melero, J. A., Morales, G., Iglesias, J. & Pizarro, P. Progress in the design of zeolite catalysts for biomass conversion into biofuels and bio-based chemicals. *Catal. Rev.* **60**, 1–70 (2018).
68. Serrano, D. P., Aguado, J. & Escola, J. M. Developing advanced catalysts for the conversion of polyolefinic waste plastics into fuels and chemicals. *ACS Catal.* **2**, 1924–1941 (2012).
69. Verboekend, D. et al. Synthesis, characterisation, and catalytic evaluation of hierarchical faujasite zeolites: milestones, challenges, and future directions. *Chem. Soc. Rev.* **45**, 3331–3352 (2016).
70. Kim, M. Y., Lee, K. & Choi, M. Cooperative effects of secondary mesoporosity and acid site location in Pt/SAPO-11 on *n*-dodecane hydroisomerization selectivity. *J. Catal.* **319**, 232–238 (2014).
71. Kim, K., Ryoo, R., Jang, H.-D. & Choi, M. Spatial distribution, strength, and dealumination behavior of acid sites in nanocrystalline MFI zeolites and their catalytic consequences. *J. Catal.* **288**, 115–123 (2012).
72. Chikkali, S. & Mecking, S. Refining of plant oils to chemicals by olefin metathesis. *Angew. Chem. Int. Ed.* **51**, 5802–5808 (2012).
73. Mol, J. C. Application of olefin metathesis in oleochemistry: an example of green chemistry. *Green Chem.* **4**, 5–13 (2002).
74. Jenkins, R. W. et al. Cross-metathesis of microbial oils for the production of advanced biofuels and chemicals. *ACS Sustain. Chem. Eng.* **3**, 1526–1535 (2015).
75. Gallo, A. et al. Ligand exchange-mediated activation and stabilization of a Re-based olefin metathesis catalyst by chlorinated alumina. *J. Am. Chem. Soc.* **138**, 12935–12947 (2016).
76. Lwin, S. & Wachs, I. E. Olefin metathesis by supported metal oxide catalysts. *ACS Catal.* **4**, 2505–2520 (2014).
77. Elevance Renewable Sciences, Inc. Elevance Renewable Sciences announces joint venture with Wilmar International to build world scale biochemical refinery. *PR Newswire* https://www.prnewswire.com/news-releases/elevance-renewable-sciences-announces-joint-venture-with-wilmar-international-to-build-world-scale-biochemical-refinery-97299669.html (2010).
78. Jia, X., Qin, C., Friedberger, T., Guan, Z. & Huang, Z. Efficient and selective degradation of polyethylenes into liquid fuels and waxes under mild conditions. *Sci. Adv.* **2**, e1501591 (2016).
79. Ellis, L. D. et al. Tandem heterogeneous catalysis for polyethylene depolymerization via an Olefin-intermediate process. *ACS Sustain. Chem. Eng.* **9**, 623–628 (2021).
80. Goldman, A. S. et al. Catalytic alkane metathesis by tandem alkane dehydrogenation-olefin metathesis. *Science* **312**, 257–261 (2006).
81. Maerten, S. et al. Glucose oxidation to formic acid and methyl formate in perfect selectivity. *Green Chem.* **22**, 4311–4320 (2020).
82. Wang, C. et al. Room temperature, near-quantitative conversion of glucose into formic acid. *Green Chem.* **21**, 6089–6096 (2019).
83. Deng, W., Zhang, Q. & Wang, Y. Catalytic transformations of cellulose and cellulose-derived carbohydrates into organic acids. *Catal. Today* **234**, 31–41 (2014).
84. Chheda, J. N. & Dumesic, J. A. An overview of dehydration, aldol-condensation and hydrogenation processes for production of liquid alkanes from biomass-derived carbohydrates. *Catal. Today* **123**, 59–70 (2007).
85. Bobbink, F. D., Zhang, J., Pierson, Y., Chen, X. & Yan, N. Conversion of chitin derived *N*-acetyl-d-glucosamine (NAG) into polyols over transition metal catalysts and hydrogen in water. *Green Chem.* **17**, 1024–1031 (2015).
86. Liang, G. et al. Production of primary amines by reductive amination of biomass-derived aldehydes/ketones. *Angew. Chem. Int. Ed.* **56**, 3050–3054 (2017).
87. Wang, C., Zhang, Q., Chen, Y., Zhang, X. & Xu, F. Highly efficient conversion of xylose residues to levulinic acid over FeCl3 catalyst in green salt solutions. *ACS Sustain. Chem. Eng.* **6**, 3154–3161 (2018).
88. Bayu, A. et al. Catalytic conversion of biomass derivatives to lactic acid with increased selectivity in an aqueous tin(II) chloride/choline chloride system. *Green Chem.* **20**, 4112–4119 (2018).
89. Wang, A. & Zhang, T. One-pot conversion of cellulose to ethylene glycol with multifunctional tungsten-based catalysts. *Acc. Chem. Res.* **46**, 1377–1386 (2013).
90. Clippel, F. et al. Fast and selective sugar conversion to alkyl lactate and lactic acid with bifunctional carbon-silica catalysts. *J. Am. Chem. Soc.* **134**, 10089–10101 (2012).
91. Holm, M. S., Saravanamurugan, S. & Taarning, E. Conversion of sugars to lactic acid derivatives using heterogeneous zeotype catalysts. *Science* **328**, 602–605 (2010).
92. Zirbes, M. et al. High-temperature electrolysis of Kraft lignin for selective vanillin formation. *ACS Sustain. Chem. Eng.* **8**, 7300–7307 (2020).
93. Kanbur, U. et al. Catalytic carbon-carbon bond cleavage and carbon-element bond formation give new life for polyolefins as biodegradable surfactants. *Chem* **7**, 1347–1362 (2021).
94. Xu, Y. et al. Research status, industrial application demand and prospects of phenolic resin. *RSC Adv.* **9**, 28924–28935 (2019).

95. Tiseo, H. Polycarbonate production capacity worldwide in 2016, by producer. *Statista* https://www.statista.com/statistics/720476/polycarbonate-global-production-capacity-distribution-by-producer/ (2021).
96. Chen, H., Wan, K., Zhang, Y. & Wang, Y. Waste to wealth: chemical recycling and chemical upcycling of waste plastics for a great future. *ChemSusChem* **14**, 4123–4136 (2021).
97. Al-Salem, S., Antelava, A., Constantinou, A., Manos, G. & Dutta, A. A review on thermal and catalytic pyrolysis of plastic solid waste (PSW). *J. Environ. Manag.* **197**, 177–198 (2017).
98. Sebestyén, Z. et al. Thermo-catalytic pyrolysis of biomass and plastic mixtures using HZSM-5. *Appl. Energy* **207**, 114–122 (2017).
99. Liao, Y., d'Halluin, M., Makshina, E., Verboekend, D. & Sels, B. F. Shape selectivity vapor-phase conversion of lignin-derived 4-ethylphenol to phenol and ethylene over acidic aluminosilicates: impact of acid properties and pore constraint. *Appl. Catal. B Environ.* **234**, 117–129 (2018).
100. Liao, Y. et al. A sustainable wood biorefinery for low-carbon footprint chemicals production. *Science* **367**, 1385–1390 (2020).
101. Chattopadhyay, J., Pathak, T., Srivastava, R. & Singh, A. Catalytic co-pyrolysis of paper biomass and plastic mixtures (HDPE (high density polyethylene), PP (polypropylene) and PET (polyethylene terephthalate)) and product analysis. *Energy* **103**, 513–521 (2016).
102. Sophonrat, N., Sandström, L., Johansson, A.-C. & Yang, W. Co-pyrolysis of mixed plastics and cellulose: an interaction study by Py-GC × GC/MS. *Energy Fuels* **31**, 11078–11090 (2017).
103. Dong, L. et al. Breaking the limit of lignin monomer production via cleavage of interunit carbon–carbon linkages. *Chem* **5**, 1521–1536 (2019).
104. Jing, Y. et al. Towards the circular economy: converting aromatic plastic waste back to arenes over a Ru/Nb2 O5 catalyst. *Angew. Chem. Int. Ed.* **60**, 5527–5535 (2021).
105. Huang, X. et al. Selective production of biobased phenol from lignocellulose-derived alkylmethoxyphenols. *ACS Catal.* **8**, 11184–11190 (2018).
106. Lu, S. et al. H2-free plastic conversion: converting PET back to BTX by unlocking hidden hydrogen. *ChemSusChem* **14**, 4242–4250 (2021).
107. Xia, Q. et al. Selective one-pot production of high-grade diesel-range alkanes from furfural and 2-methylfuran over Pd/NbOPO4. *ChemSusChem* **10**, 747–753 (2017).
108. Xin, Y. et al. Selective production of indane and its derivatives from lignin over a modified niobium-based catalyst. *Chem. Commun.* **55**, 9391–9394 (2019).
109. Verboekend, D., Liao, Y., Schutyser, W. & Sels, B. F. Alkylphenols to phenol and olefins by zeolite catalysis: a pathway to valorize raw and fossilized lignocellulose. *Green Chem.* **18**, 297–306 (2016).
110. Wang, M. et al. Dealkylation of lignin to phenol via oxidation–hydrogenation strategy. *ACS Catal.* **8**, 6837–6843 (2018).
111. Dong, L. et al. Mechanisms of caromatic-C bonds cleavage in lignin over NbOx-supported Ru catalyst. *J. Catal.* **394**, 94–103 (2021).
112. Li, S. et al. Selective hydrogenation of 5-(hydroxymethyl)furfural to 5-methylfurfural over single atomic metals anchored on Nb_2O_5. *Nat. Commun.* **12**, 584 (2021).
113. Yan, J. et al. Selective valorization of lignin to phenol by direct transformation of Csp2–Csp3 and C–O bonds. *Sci. Adv.* **6**, eabd1951 (2020).
114. Zhu, J., Wang, J. & Dong, G. Catalytic activation of unstrained C(aryl)-C(aryl) bonds in 2,2′-biphenols. *Nat. Chem.* **11**, 45–51 (2019).
115. Zakzeski, J. & Weckhuysen, B. M. Lignin solubilization and aqueous phase reforming for the production of aromatic chemicals and hydrogen. *ChemSusChem* **4**, 369–378 (2011).
116. Shuai, L. et al. Selective C–C bond cleavage of methylene-linked lignin models and kraft lignin. *ACS Catal.* **8**, 6507–6512 (2018).
117. Che, P. et al. Hydrogen bond distinction and activation upon catalytic etherification of hydroxyl compounds. *Chem. Commun.* **51**, 1077–1080 (2015).
118. Mordor Intelligence. Epoxy resins market — growth, trends, COVID-19 impact, and forecasts (2022–2027). *Mordor Intelligence* https://www.mordorintelligence.com/industry-reports/global-epoxy-resin-market-industry (2021).
119. Acute Market Reports. Global polyphenylene oxide (PPO) resins market size & share, application analysis, regional outlook, growth trends, key players, competitive strategies and forecasts to 2026. *Research and Markets* https://www.researchandmarkets.com/research/75xn3c/global?w=4 (2018).
120. Jing, Y., Dong, L., Guo, Y., Liu, X. & Wang, Y. Chemicals from lignin: a review of catalytic conversion involving hydrogen. *ChemSusChem* **13**, 4181–4198 (2020).
121. Zhang, J., Sun, J. & Wang, Y. Recent advances in the selective catalytic hydrodeoxygenation of lignin-derived oxygenates to arenes. *Green Chem.* **22**, 1072–1098 (2020).
122. Chiu, C.-c, Genest, A., Borgna, A. & Rösch, N. Hydrodeoxygenation of guaiacol over Ru(0001): a DFT study. *ACS Catal.* **4**, 4178–4188 (2014).
123. Shi, D., Arroyo-Ramírez, L. & Vohs, J. M. The use of bimetallics to control the selectivity for the upgrading of lignin-derived oxygenates: reaction of anisole on Pt and PtZn catalysts. *J. Catal.* **340**, 219–226 (2016).
124. Shi, D. & Vohs, J. M. Deoxygenation of biomass-derived oxygenates: reaction of furfural on Zn-modified Pt(111). *ACS Catal.* **5**, 2177–2183 (2015).
125. Ma, D., Lu, S., Liu, X., Guo, Y. & Wang, Y. Depolymerization and hydrodeoxygenation of lignin to aromatic hydrocarbons with a Ru catalyst on a variety of Nb-based supports. *Chin. J. Catal.* **40**, 609–617 (2019).
126. Yang, F. et al. Size dependence of vapor phase hydrodeoxygenation of *m*-cresol on Ni/SiO_2 catalysts. *ACS Catal.* **8**, 1672–1682 (2018).
127. Mondelli, C., Gozaydin, G., Yan, N. & Perez-Ramirez, J. Biomass valorisation over metal-based solid catalysts from nanoparticles to single atoms. *Chem. Soc. Rev.* **49**, 3764–3782 (2020).
128. Kim, S. et al. Recent advances in hydrodeoxygenation of biomass-derived oxygenates over heterogeneous catalysts. *Green Chem.* **21**, 3715–3743 (2019).
129. Zhang, C. & Wang, F. Catalytic lignin depolymerization to aromatic chemicals. *Acc. Chem. Res.* **53**, 470–484 (2020).
130. Zeng, H., Cao, D., Qiu, Z. & Li, C. J. Palladium-catalyzed formal cross-coupling of diaryl ethers with amines: slicing the 4-O-5 linkage in lignin models. *Angew. Chem. Int. Ed.* **57**, 3752–3757 (2018).
131. Wong, S. S., Shu, R., Zhang, J., Liu, H. & Yan, N. Downstream processing of lignin derived feedstock into end products. *Chem. Soc. Rev.* **49**, 5510–5560 (2020).
132. Wang, M., Shi, H., Camaioni, D. M. & Lercher, J. A. Palladium-catalyzed hydrolytic cleavage of aromatic C–O bonds. *Angew. Chem. Int. Ed.* **56**, 2110–2114 (2017).
133. Shao, Y. et al. Selective production of arenes via direct lignin upgrading over a niobium-based catalyst. *Nat. Commun.* **8**, 16104 (2017).
134. Shu, R. et al. A review on the catalytic hydrodeoxygenation of lignin-derived phenolic compounds and the conversion of raw lignin to hydrocarbon liquid fuels. *Biomass Bioenergy* **132**, 105432 (2020).
135. Kong, J., He, M., Lercher, J. A. & Zhao, C. Direct production of naphthenes and paraffins from lignin. *Chem. Commun.* **51**, 17580–17583 (2015).
136. Dong, L. et al. Comparison of two multifunctional catalysts [M/Nb_2O_5 (M=Pd, Pt)] for one-pot hydrodeoxygenation of lignin. *Catal. Sci. Technol.* **8**, 6129–6136 (2018).
137. Mao, J. et al. Anatase TiO_2 activated by gold nanoparticles for selective hydrodeoxygenation of guaiacol to phenolics. *ACS Catal.* **7**, 695–705 (2017).
138. Liu, K. et al. Silver initiated hydrogen spillover on anatase TiO_2 creates active sites for selective hydrodeoxygenation of guaiacol. *J. Catal.* **369**, 396–404 (2019).
139. Li, H., Bunrit, A., Li, N. & Wang, F. Heteroatom-participated lignin cleavage to functionalized aromatics. *Chem. Soc. Rev.* **49**, 3748–3763 (2020).
140. Cao, D., Zeng, H. & Li, C.-J. Formal cross-coupling of diaryl ethers with ammonia by dual C(Ar)–O bond cleavages. *ACS Catal.* **8**, 8873–8878 (2018).
141. Fedorov, A., Toutov, A. A., Swisher, N. A. & Grubbs, R. H. Lewis-base silane activation: from reductive cleavage of aryl ethers to selective ortho-silylation. *Chem. Sci.* **4**, 1640–1645 (2013).
142. Ren, Y., Yan, M., Wang, J., Zhang, Z. C. & Yao, K. Selective reductive cleavage of inert aryl C–O bonds by an iron catalyst. *Angew. Chem. Int. Ed.* **52**, 12674–12678 (2013).
143. Wu, W. B. & Huang, J. M. Electrochemical cleavage of aryl ethers promoted by sodium borohydride. *J. Org. Chem.* **79**, 10189–10195 (2014).
144. He, J. et al. Sustainable access to renewable N-containing chemicals from reductive amination of biomass-derived platform compounds. *Green Chem.* **22**, 6714–6747 (2020).
145. Wang, Y., Furukawa, S., Fu, X. & Yan, N. Organonitrogen chemicals from oxygen-containing feedstock over heterogeneous catalysts. *ACS Catal.* **10**, 311–335 (2019).
146. Movil-Cabrera, O., Rodriguez-Silva, A., Arroyo-Torres, C. & Staser, J. A. Electrochemical conversion of lignin to useful chemicals. *Biomass Bioenergy* **88**, 89–96 (2016).
147. Garedew, M. et al. Electrocatalytic cleavage of lignin model dimers using ruthenium supported on activated carbon cloth. *Sustain. Energy Fuels* **4**, 1340–1350 (2020).
148. Yang, F., Zhang, Q., Fan, H.-X., Li, Y. & Li, G. Electrochemical control of the conversion of cellulose oligosaccharides into glucose. *J. Ind. Eng. Chem.* **20**, 3487–3492 (2014).
149. Sanyal, U., Lopez-Ruiz, J., Padmaperuma, A. B., Holladay, J. & Gutiérrez, O. Y. Electrocatalytic hydrogenation of oxygenated compounds in aqueous phase. *Org. Process. Res. Dev.* **22**, 1590–1598 (2018).
150. Song, Y., Chia, S. H., Sanyal, U., Gutiérrez, O. Y. & Lercher, J. A. Integrated catalytic and electrocatalytic conversion of substituted phenols and diaryl ethers. *J. Catal.* **344**, 263–272 (2016).
151. Rahimi, A., Ulbrich, A., Coon, J. J. & Stahl, S. S. Formic-acid-induced depolymerization of oxidized lignin to aromatics. *Nature* **515**, 249–252 (2014).
152. Rahimi, A., Azarpira, A., Kim, H., Ralph, J. & Stahl, S. S. Chemoselective metal-free aerobic alcohol oxidation in lignin. *J. Am. Chem. Soc.* **135**, 6415–6418 (2013).
153. Lancefield, C. S., Ojo, O. S., Tran, F. & Westwood, N. J. Isolation of functionalized phenolic monomers through selective oxidation and C–O bond cleavage of the beta-O-4 linkages in lignin. *Angew. Chem. Int. Ed.* **54**, 258–262 (2015).
154. Cai, Z. et al. Selective production of diethyl maleate via oxidative cleavage of lignin aromatic unit. *Chem* **5**, 2365–2377 (2019).
155. Dai, J., Gözaydın, G., Hu, C. & Yan, N. Catalytic conversion of chitosan to glucosaminic acid by tandem hydrolysis and oxidation. *ACS Sustain. Chem. Eng.* **7**, 12399–12407 (2019).
156. Yang, Y. et al. Conversion of cellulose to high-yield glucose in water over sulfonated mesoporous carbon fibers with optimized acidity. *Green Chem.* **23**, 4477–4489 (2021).
157. Li, O. L., Ikura, R. & Ishizaki, T. Hydrolysis of cellulose to glucose over carbon catalysts sulfonated via a plasma process in dilute acids. *Green Chem.* **19**, 4774–4777 (2017).
158. Chen, P., Shrotri, A. & Fukuoka, A. Soluble cello-oligosaccharides produced by carbon-catalyzed hydrolysis of cellulose. *ChemSusChem* **12**, 2576–2580 (2019).
159. Cai, H., Li, C., Wang, A., Xu, G. & Zhang, T. Zeolite-promoted hydrolysis of cellulose in ionic liquid, insight into the mutual behavior of zeolite, cellulose and ionic liquid. *Appl. Catal. B Environ.* **123**, 333–338 (2012).
160. Zhong, J., Pérez-Ramírez, J. & Yan, N. Biomass valorisation over polyoxometalate-based catalysts. *Green Chem.* **23**, 18–36 (2021).
161. Huo, F., Liu, Z. & Wang, W. Cosolvent or antisolvent? A molecular view of the interface between ionic liquids and cellulose upon addition of another molecular solvent. *J. Phys. Chem. B* **117**, 11780–11792 (2013).
162. Andanson, J.-M. et al. Understanding the role of co-solvents in the dissolution of cellulose in ionic liquids. *Green Chem.* **16**, 2528–2538 (2014).
163. Zhang, X., Qu, T., Mosier, N. S., Han, L. & Xiao, W. Cellulose modification by recyclable swelling solvents. *Biotechnol. Biofuels* **11**, 191 (2018).
164. Zhang, L., Huang, C., Zhang, C. & Pan, H. Swelling and dissolution of cellulose in binary systems of three ionic liquids and three co-solvents. *Cellulose* **28**, 4643–4653 (2021).
165. Gözaydın, G., Song, S. & Yan, N. Chitin hydrolysis in acidified molten salt hydrates. *Green Chem.* **22**, 5096–5104 (2020).
166. Luo, Y.-R. *Comprehensive Handbook of Chemical Bond Energies* (CRC Press, 2007).
167. Canakci, M. & Van Gerpen, J. Biodiesel production via acid catalysis. *Trans. ASAE* **42**, 1203–1210 (1999).
168. Tamura, M., Nakagawa, Y. & Tomishige, K. Recent developments of heterogeneous catalysts for hydrogenation of carboxylic acids to their corresponding alcohols. *Asian J. Org. Chem.* **9**, 126–143 (2020).
169. Pham, D. D. & Cho, J. Low-energy catalytic methanolysis of poly(ethyleneterephthalate). *Green Chem.* **23**, 511–525 (2021).

170. Fernandes, J. R., Amaro, L. P., Muniz, E. C., Favaro, S. L. & Radovanovic, E. PET depolimerization in supercritical ethanol conditions catalysed by nanoparticles of metal oxides. *J. Supercrit. Fluids* **158**, 104715 (2020).
171. Wang, H., Li, Z., Liu, Y., Zhang, X. & Zhang, S. Degradation of poly(ethylene terephthalate) using ionic liquids. *Green Chem.* **11**, 1568–1575 (2009).
172. Iannone, F. et al. Ionic liquids/ZnO nanoparticles as recyclable catalyst for polycarbonate depolymerization. *J. Mol. Catal. A Chem.* **426**, 107–116 (2017).
173. Al-Sabagh, A. M. et al. Glycolysis of poly(ethylene terephthalate) catalyzed by the Lewis base ionic liquid [Bmim][OAc]. *Ind. Eng. Chem. Res.* **53**, 18443–18451 (2014).
174. Ullah, Z., Bustam, M. A. & Man, Z. Biodiesel production from waste cooking oil by acidic ionic liquid as a catalyst. *Renew. Energy* **77**, 521–526 (2015).
175. Leadbeater, N. E. & Stencel, L. M. Fast, easy preparation of biodiesel using microwave heating. *Energy Fuels* **20**, 2281–2283 (2006).
176. Parab, Y. S., Pingale, N. D. & Shukla, S. R. Aminolytic depolymerization of poly (ethylene terephthalate) bottle waste by conventional and microwave irradiation heating. *J. Appl. Polym. Sci.* **125**, 1103–1107 (2012).
177. Goto, M., Sasaki, M. & Hirose, T. Reactions of polymers in supercritical fluids for chemical recycling of waste plastics. *J. Mater. Sci.* **41**, 1509–1515 (2006).
178. Saka, S. & Kusdiana, D. Biodiesel fuel from rapeseed oil as prepared in supercritical methanol. *Fuel* **80**, 225–231 (2001).
179. Bhogle, C. S. & Pandit, A. B. Ultrasound assisted methanolysis of polycarbonate at room temperature. *Ultrason. Sonochem.* **58**, 104667 (2019).
180. Boffito, D. C. et al. Ultrafast biodiesel production using ultrasound in batch and continuous reactors. *ACS Sustain. Chem. Eng.* **1**, 1432–1439 (2013).
181. PET Monomer Recycling Special Industry Group. PET monomer recycling SIG primary members. *Petcore Europe* https://www.petmonomerrecycling.org/members (2019).
182. Tullo, A. H. Eastman will build a $250 million plastics recycling plant. *Chemical & Engineering News* https://cen.acs.org/environment/recycling/Eastman-build-250-million-plastics/99/web/2021/02 (2021).
183. Zhou, H. et al. Electrocatalytic upcycling of polyethylene terephthalate to commodity chemicals and H_2 fuel. *Nat. Commun.* **12**, 4679 (2021).
184. Arturi, K. R. et al. Recovery of value-added chemicals by solvolysis of unsaturated polyester resin. *J. Clean. Prod.* **170**, 131–136 (2018).
185. Kubičková, I., Snåre, M., Eränen, K., Mäki-Arvela, P. & Murzin, D. Y. Hydrocarbons for diesel fuel via decarboxylation of vegetable oils. *Catal. Today* **106**, 197–200 (2005).
186. Peng, B., Yuan, X., Zhao, C. & Lercher, J. A. Stabilizing catalytic pathways via redundancy: selective reduction of microalgae oil to alkanes. *J. Am. Chem. Soc.* **134**, 9400–9405 (2012).
187. Kratish, Y., Li, J., Liu, S., Gao, Y. & Marks, T. J. Polyethylene terephthalate deconstruction catalyzed by a carbon-supported single-site molybdenum-dioxo complex. *Angew. Chem. Int. Ed.* **59**, 19857–19861 (2020).
188. Krall, E. M. et al. Controlled hydrogenative depolymerization of polyesters and polycarbonates catalyzed by ruthenium(II) PNN pincer complexes. *Chem. Commun.* **50**, 4884–4887 (2014).
189. Westhues, S., Idel, J. & Klankermayer, J. Molecular catalyst systems as key enablers for tailored polyesters and polycarbonate recycling concepts. *Sci. Adv.* **4**, eaat9669 (2018).
190. Kreutzer, U. R. Manufacture of fatty alcohols based on natural fats and oils. *J. Am. Oil Chem. Soc.* **61**, 343–348 (1984).
191. Ikeda, M. & Takeno, S. in *Corynebacterium glutamicum: Biology and Biotechnology* (eds Inui, M. & Toyoda, K.) 175–226 (Springer, 2012).
192. Global Industry Analysts, Inc. Nylon — global market trajectory & analytics. *Research and Markets* http://www.researchandmarkets.com/reports/1227800/nylon_global_market_trajectory_and_analytics (2021).
193. Fernández, L. Global polyurethane market volume 2015–2021. *Statista* https://www.statista.com/statistics/720341/global-polyurethane-market-size-forecast/ (2021).
194. Chen, X. & Yan, N. in *Chemical Catalysts for Biomass Upgrading* (eds Crocker, M. & Santillan-Jimenez E.) 569–590 (Wiley-VCH, 2020).
195. Ma, X. et al. Upcycling chitin-containing waste into organonitrogen chemicals via an integrated process. *Proc. Natl Acad. Sci. USA* **117**, 7719–7728 (2020).
196. Cabrero-Antonino, J. R., Adam, R., Papa, V. & Beller, M. Homogeneous and heterogeneous catalytic reduction of amides and related compounds using molecular hydrogen. *Nat. Commun.* **11**, 3893 (2020).
197. Kim, K. J., Dhevi, D. M., Lee, J. S., Cho, Y. D. & Choe, E. K. Mechanism of glycolysis of nylon 6,6 and its model compound by ethylene glycol. *Polym. Degrad. Stab.* **91**, 1545–1555 (2006).
198. Klun, U. & Kržan, A. Rapid microwave induced depolymerization of polyamide-6. *Polymer* **41**, 4361–4365 (2000).
199. Shukla, S. R., Harad, A. M. & Mahato, D. Depolymerization of nylon 6 waste fibers. *J. Appl. Polym. Sci.* **100**, 186–190 (2006).
200. Cesarek, U., Pahovnik, D. & Zagar, E. Chemical recycling of aliphatic polyamides by microwave-assisted hydrolysis for efficient monomer recovery. *ACS Sustain. Chem. Eng.* **8**, 16274–16282 (2020).
201. Kamimura, A. & Yamamoto, S. An efficient method to depolymerize polyamide plastics: a new use of ionic liquids. *Org. Lett.* **9**, 2533–2535 (2007).
202. Kamimura, A., Oishi, Y., Kaiso, K., Sugimoto, T. & Kashiwagi, K. Supercritical secondary alcohols as useful media to convert polyamide into monomeric lactams. *ChemSusChem* **1**, 82–84 (2008).
203. Sari, Y. W., Alting, A. C., Floris, R., Sanders, J. P. M. & Bruins, M. E. Glutamic acid production from wheat by-products using enzymatic and acid hydrolysis. *Biomass Bioenergy* **67**, 451–459 (2014).
204. Fountoulakis, M. & Lahm, H.-W. Hydrolysis and amino acid composition analysis of proteins. *J. Chromatogr. A* **826**, 109–134 (1998).
205. Ito, M. et al. Hydrogenation of *N*-acylcarbamates and *N*-acylsulfonamides catalyzed by a bifunctional [Cp*Ru(PN)] complex. *Angew. Chem. Int. Ed.* **48**, 1324–1327 (2009).
206. Balaraman, E., Gnanaprakasam, B., Shimon, L. J. W. & Milstein, D. Direct hydrogenation of amides to alcohols and amines under mild conditions. *J. Am. Chem. Soc.* **132**, 16756–16758 (2010).
207. Cabrero-Antonino, J. R. et al. Efficient base-free hydrogenation of amides to alcohols and amines catalyzed by well-defined pincer imidazolyl–ruthenium complexes. *ACS Catal.* **6**, 47–54 (2016).
208. Garg, J. A., Chakraborty, S., Ben-David, Y. & Milstein, D. Unprecedented iron-catalyzed selective hydrogenation of activated amides to amines and alcohols. *Chem. Commun.* **52**, 5285–5288 (2016).
209. Papa, V. et al. Efficient and selective hydrogenation of amides to alcohols and amines using a well-defined manganese–PNN pincer complex. *Chem. Sci.* **8**, 3576–3585 (2017).
210. Xie, Y., Hu, P., Bendikov, T. & Milstein, D. Heterogeneously catalyzed selective hydrogenation of amides to alcohols and amines. *Catal. Sci. Technol.* **8**, 2784–2788 (2018).
211. Tamura, M., Ishikawa, S., Betchaku, M., Nakagawa, Y. & Tomishige, K. Selective hydrogenation of amides to alcohols in water solvent over a heterogeneous CeO_2-supported Ru catalyst. *Chem. Commun.* **54**, 7503–7506 (2018).
212. Sorribes, I. et al. Palladium doping of In_2O_3 towards a general and selective catalytic hydrogenation of amides to amines and alcohols. *Catal. Sci. Technol.* **9**, 6965–6976 (2019).
213. Kumar, A. et al. Hydrogenative depolymerization of nylons. *J. Am. Chem. Soc.* **142**, 14267–14275 (2020).
214. Demirbas, A. & Arin, G. An overview of biomass pyrolysis. *Energy Sources* **24**, 471–482 (2002).
215. Williams, P. T. & Nugranad, N. Comparison of products from the pyrolysis and catalytic pyrolysis of rice husks. *Energy* **25**, 493–513 (2000).
216. Kan, T., Strezov, V. & Evans, T. J. Lignocellulosic biomass pyrolysis: a review of product properties and effects of pyrolysis parameters. *Renew. Sustain. Energy Rev.* **57**, 1126–1140 (2016).
217. Kaminsky, W., Schlesselmann, B. & Simon, C. Olefins from polyolefins and mixed plastics by pyrolysis. *J. Anal. Appl. Pyrolysis* **32**, 19–27 (1995).
218. Lopez, A., de Marco, I., Caballero, B. M., Laresgoiti, M. F. & Adrados, A. Pyrolysis of municipal plastic wastes: influence of raw material composition. *Waste Manag.* **30**, 620–627 (2010).
219. Chen, D., Yin, L., Wang, H. & He, P. Pyrolysis technologies for municipal solid waste: a review. *Waste Manag.* **34**, 2466–2486 (2014).
220. Sutton, D., Kelleher, B. & Ross, J. R. H. Review of literature on catalysts for biomass gasification. *Fuel Process. Technol.* **73**, 155–173 (2001).
221. Lv, P. et al. Hydrogen-rich gas production from biomass air and oxygen/steam gasification in a downdraft gasifier. *Renew. Energy* **32**, 2173–2185 (2007).
222. Snehesh, A. S., Mukunda, H. S., Mahapatra, S. & Dasappa, S. Fischer-tropsch route for the conversion of biomass to liquid fuels — technical and economic analysis. *Energy* **130**, 182–191 (2017).
223. Ponzio, A., Kalisz, S. & Blasiak, W. Effect of operating conditions on tar and gas composition in high temperature air/steam gasification (HTAG) of plastic containing waste. *Fuel Process. Technol.* **87**, 223–233 (2006).
224. Wu, C. & Williams, P. T. Hydrogen production by steam gasification of polypropylene with various nickel catalysts. *Appl. Catal. B Environ.* **87**, 152–161 (2009).
225. Salaudeen, S., Arku, P. & Dutta, A. in *Plastics to Energy* (Ed. Al-Salem, S. M.) 269–293 (Elsevier, 2019).
226. Zhuo, C. & Levendis, Y. A. Upcycling waste plastics into carbon nanomaterials: a review. *J. Appl. Polym. Sci.* **131**, 39931 (2014).
227. Wang, Z., Shen, D., Wu, C. & Gu, S. State-of-the-art on the production and application of carbon nanomaterials from biomass. *Green Chem.* **20**, 5031–5057 (2018).
228. Gao, Y., Chen, X., Zhang, J. & Yan, N. Chitin derived mesoporous, nitrogen-containing carbon for heavy metal removal and styrene epoxidation. *ChemPlusChem* **80**, 1556–1564 (2015).

Acknowledgements
The authors thank the National Research Foundation of Singapore NRF Investigatorship (award no.: NRF-NRFI07-2021-0006), National Research Foundation of Singapore under its Campus for Research Excellence and Technological Enterprise (CREATE) programme (CARES), Emerging Opportunities Fund-EOF2 (Chemical Farming, WBS R-279-000-604-592), the National Natural Science Foundation of China (no. 21832002), the Science and Technology Commission of Shanghai Municipality (2018SHZDZX03) and the project funded by China Postdoctoral Science Foundation (2021M691011 and 2021TQ0106).

Author contributions
N.Y. conceived the Review. K.L. and Y.J. conducted the literature search and prepared the manuscript. Y.W. and N.Y. supervised the project and revised the manuscript. All authors participated in discussions.

Competing interests
The authors declare no competing interests.

Peer review information
Nature Reviews Chemistry thanks Ye Wang and the other anonymous reviewer(s) for their contribution to the peer review of this work.

Publisher's note
Springer Nature remains neutral with regard to jurisdictional claims in published maps and institutional affiliations.